De-noising of Hyper-spectral Images in Wavelet Domain with Improved Soft Thresholding

Noorbakhsh Amiri Golilarz

Submitted to the
Institute of Graduate Studies and Research
in partial fulfillment of the requirements for the Degree of

Master of Science
in
Electrical and Electronic Engineering

Eastern Mediterranean University
January 2017
Gazimağusa, North Cyprus

Approval of the Institute of Graduate Studies and Research

Prof. Dr. Mustafa Tümer
Director

I certify that this thesis satisfies the requirements as a thesis for the degree of Master of Science in Electrical and Electronic Engineering.

Prof. Dr. Hasan Demirel
Chair, Department of Electrical and Electronic Engineering

We certify that we have read this thesis and that in our opinion it is fully adequate in scope and quality as a thesis for the degree of Master of Science in Electrical and Electronic Engineering.

Prof. Dr. Hasan Demirel
Supervisor

Examining Committee

1. Prof. Dr. Hasan Demirel _____

2. Assoc. Prof. Dr. Önsen Toygar _____

3. Asst. Prof. Dr. Rasime Uyguroğlu _____

ABSTRACT

A hyper-spectral image can be corrupted by noise during the transmission process. The noise does not have positive effect on the image, so it is essential to discard the noise before performing analysis to improve the quality of an image. Noise removal is among the important and challenging works for scientists and researchers in the field of image processing. The main objective of noise removal is to enhance the visual quality of the noisy using de-noising techniques. That is why researchers try to discard the noise before they perform further analysis.

The main focus of the thesis is removing noise from hyper-spectral remote sensing images. Image de-nosing helps us improve the quality of the image, so we are able to analyze the image properly. In this thesis, we use 2D and 3D-DWT combined with hard and soft thresholding for de-noising hyper-spectral images. De-noising based on DWT introduces weakness such as lack of translation invariance. That is why; we suggest using Un-decimated Wavelet Transform (UWT) which discards the mentioned problem. Additionally, 2D and 3D-UWT with soft and hard thresholding functions were used as part of the proposed de-noising techniques.

Finally we propose to use a new method for image de-noising in wavelet domain based on applying a smooth nonlinear soft threshold function on Un-decimated Wavelet Transform. This higher order threshold function is known as the improved soft thresholding function. Here we combined this function with 2D and 3D-UWT. Comparing the performance analysis between 2D-UWT and 3D-UWT using improved soft threshold function shows that 3D version outperforms 2D in terms of

PSNR value and visual quality. This technique provides us with higher quality and improvement in PSNR value in comparison with several other methods available for de-noising. The proposed method achieves PSNR improvement by 2.12 dB for band 25 of Indian Pine, 1.29 dB for Cuprite Mining District image, 1.46 dB for Arizona Mining and 1.17dB for Golf of Mexico over de-noising based on 3D-UWT with standard soft thresholding technique.

Keywords: Hyperspectral image de-noising, wavelet transform, hard and soft thresholding.

ÖZ

Hiper-spektral bir görüntü, iletim işlemi sırasında gürültü ile bozulabilir. Gürültünün görüntü üzerinde olumlu etkisi yoktur; bu nedenle, bir görüntünün kalitesini artırmak için analiz gerçekleştirmeden önce gürültüyü atmanız önemlidir. Gürültü giderme, görüntü işleme alanında bilimadamları ve araştırmacılar için önemli ve zorlu çalışmalar arasındadır. Gürültünün ortadan kaldırılmasının asıl amacı, gürültü azaltma teknikleri kullanarak gürültünün görsel kalitesini arttırmaktır. Genellikle, araştırmacılar daha fazla analiz yapmadan önce gürültüyü atmaya çalışırlar.

Bu tezin ana odağı hiper-spektral uzaktan algılama görüntülerinden gelen gürültünün giderilmesidir. İmge gürültü giderme işlemi görüntünün kalitesini artırmamıza ve sonrasında görüntüleri doğru analiz edebilmemize yardımcı olur. Bu tezde, 2D ve 3D-DWT'yi, hiper-spektral görüntülerin gürültüsüzleştirilmesi için sert ve yumuşak eşikleme işleminde birlikte edilerek kullanıyoruz. DWT'ye dayanan gürültü önleme, kaydırma değişmezlik özelliğinin olmaması gibi zayıflıkları ortaya çıkarmaktadır. Bu yüzden; bahsedilen problemi ortadan kaldıran kırımsız dalgacık dönüşümü (UWT) kullanmayı öneriyoruz. Ayrıca, önerilen gürültü azaltma tekniklerinin bir parçası olarak yumuşak ve sert eşikleme işlevlerine sahip 2D ve 3D-UWT kullanılmıştır.

Son olarak, kırımsız dalgacık dönüşümü (UWT) üzerinde pürüzsüz bir doğrusal olmayan yumuşak eşik fonksiyonu uygulanmasına dayanan dalgacık alanında görüntü sönümlemesi için yeni bir yöntem kullanmayı öneriyoruz. Bu yüksek dereceden eşik fonksiyonu gelişmiş yumuşak eşik fonksiyonu olarak bilinir. Geliştirilmiş yumuşak eşik fonksiyonunu kullanarak 2D-UWT ve 3D-UWT

arasındaki performans analizinin karşılaştırılması, 3D versiyonun PSNR değeri ve görsel kalite bakımından 2D'den daha iyi performans gösterdiğini gösterir. Bu teknik, gürültü azaltma için kullanılabilecek alternatif yöntemlerle karşılaştırıldığında, PSNR değerinde daha yüksek kalite ve iyileşme sağlanmaktadır. Önerilen yöntem, standart yumuşak eşikleme tekniği ile 3D-UWT'ye dayanan de-noising üzerinde Indian Pine 25 bandı için 2.12 dB, Cuprite Madencilik Bölgesi görüntüsü için 1.29 dB, Arizona Madencilik için 1.46 dB ve Golf Golf için 1.17dB PSNR iyileştirmesine ulaşmaktadır.

Anahtar Kelimeler: Hiperspektral gürültü çıkarımı, dalgacık dönüşümü, sert ve yumuşak eşikleme.

DEDICATION

To My Family and My Dear Wife

ACKNOWLEDGMENT

I would like to record my gratitude to Prof. Dr. Hasan Demirel for his supervision, advice, and guidance from the very early stage of this thesis as well as giving me extraordinary experiences throughout the work. Above all and the most needed, he provided me constant encouragement and support in various ways. His ideas, experiences, and passions have truly inspired and enrich my growth as a student. I am indebted to him more than he knows.

My thanks go to my family who helped and encouraged me to continue my higher education in Cyprus. I deeply appreciate my family for supporting me both emotionally and financially.

Last but not least, I would like to thanks my wife in advance who always motivated me during my studies. I need to express my deepest appreciation to her because of her patience during my research.

TABLE OF CONTENTS

LIST OF TABLES

LIST OF FIGURES

LIST OF SYMBOLS

k	Order of the Improved Soft Threshold Function
$P_H(\omega)$	Hard Threshold Function
$P_S(\omega)$	Soft Threshold Function
σ	Standard Deviation
T	Threshold Value
$T_I(\omega)$	Improved Soft Threshold Function
ω	Wavelet Coefficients

LIST OF ABBREVIATIONS

AC	Approximation Coefficients
AVIRIS	Airborne Visible / Infrared Imaging Spectrometer
AWGN	Additive White Gaussian Noise
DC	Detail Coefficients
DWT	Discrete Wavelet Transform
H	High Pass
IDWT	Inverse Discrete Wavelet Transform
L	Low Pass
MSE	Mean Square Error
PSNR	Peak Signal to Noise Ratio
ROSIS	Reflective Optics System Imaging Spectrometer
3D-DWT	Three Dimensional Discrete Wavelet Transform
3D-UWT	Three Dimensional Un-decimated Wavelet Transform
2D-DWT	Two Dimensional Discrete Wavelet Transform
2D-UWT	Two Dimensional Un-decimated Wavelet Transform
UWT	Un-decimated Wavelet Transform
WDM	Washington DC Mall

Chapter 1

INTRODUCTION

1.1 Introduction

While capability of digital imaging and spectroscopy (creation and observation of colors of a spectrum through a spectroscope) join together, hyper-spectral imaging will be obtained [1]. In hyper-spectral imaging, all data can be advanced upon the electromagnetic spectrum [2]. In addition, each pixel in the image includes a continuous spectrum which is because of obtaining the light intensity for a wide variety of contiguous spectral bands [1]. Different types of sensors like AVIRIS (Airborne Visible / Infrared Imaging Spectrometer) and ROSIS (Reflective Optics System Imaging Spectrometer) are very useful to capture hyper-spectral images.

Human beings can see objects having wavelength of 400-700 nm (between infrared and ultraviolet) in three bands (red, green and blue) [3] but spectral imaging apportion the spectrum into many bands, which definitely can be extended beyond the visible, so this kind of imaging contains a wide domain of wavelength.

These types of images include spectral/spatial data. Some of these spectral bands may be affected by noise during their acquisition and transmission process, so removing noise from these corrupted bands is kind of important works in image processing. Nowadays, de-noising with wavelet transform is a method which many of researchers are focusing on it by choosing the proper threshold value to remove

noisy coefficients from cited images to have a clean version of image [4]. De-noising provides us with a reconstructed image which lots of most important information have retained. That is why de-noising is one of the most important tasks in image processing.

1.2 Problem Definition

1.2.1 Additive White Gaussian Noise (AWGN) in Hyper-spectral Images

Noise is defined as the deviation of image resolution which is usually random and does not have any specific pattern. This noise can contaminate the resolution of image which results in diminishing the visual inspection. It can be obtained by sensor, digital camera, scanner and bad environment conditions (snow and rain) [5]. When our image is corrupted by noise, we can see many dots in our image which it means that the resolution of our image is decreased, moreover; some important features will be lost and as a result, we will have an image with low resolution. According to low resolution of noisy image, de-noising method is needed to retain some of those important features to increase the resolution of image. Different noise models are as the following: Gaussian Noise, Salt and Pepper noise, Peckle Noise, Periodic Noise, Quantization Noise, Poison Noise, Gamma Noise and Rayleigh Noise [6]. Here AWGN is used in this thesis. Presence of this type of noise results in influencing or contamination of each pixel of an image. The general idea and formula is mentioned in (1.2) properly.

1.2.2 Effect of Noise on Images

An Image can be influenced by noise while sending and receiving process. This noise can be as White Gaussian Additive Noise corrupting images in the mentioned phases. Unfortunately, these effects can influence the resolution of image and reduce

its performance. It is clearly proof enough that the resolution of original image has declined due to presence of noise.

Following formula shows the affecting of noise on original image:

$$g(x,y) = f(x,y) * h(x,g) + \eta(x,y) \quad 1 < (x,y) < n \qquad (1.1)$$

Where $g(x,y)$ is our image influenced by noise, $f(x,y)$ is original image, $h(x,y)$ is degradation function which can be ignored and then we can write the above formula as:

$$g(x,y) = f(x,y) + \eta(x,y) \quad 1 < (x,y) < n \qquad (1.2)$$

where $\eta(x,y) \sim N(0,\sigma^2)$ is Additive White Gaussian Noise with zero mean and variance σ^2 [7].

1.2.3 Noise Removal in Hyper-spectral Images

In terms of hyper-spectral images, noise repression is kind of very important works. Hyper-spectral image acquisition and transmission process may be accompanied by high occurrence of noise, so target detection, classification and segmentation will be highly influenced by noise [8]. A plus point is that, analyzing these images cannot be properly done except by some types of noise removal techniques.

Wavelet domain image de-noising is one of the common methods for noise removing. De-noising using wavelet transform requires some threshold value to discard those types of coefficients which are not important (noisy wavelet coefficients) and keep crucial coefficients which hold important features of image [9]. This step is followed by determining threshold function which soft and hard thresholding functions are the most common functions we can use. Here improved

soft threshold function is proposed in this thesis to enhance the resolution and increase the amount of PSNR in comparison with other techniques.

1.3 Wavelet Transform Based Noise Removal

The main purpose of wavelet de-noising technique is to get a reconstructed image from noisy level. Here proper threshold value is needed to discard small coefficients which are considered as noisy coefficients and keep large coefficients which hold main features of our image [9],[10]. Plenty methods have introduced for de-noising images based on wavelet transform. Demir and Ertrk proposed a method to de-noise hyper-spectral images band by band [11]. Another method is based on spectral domain noise reduction [12]. In [13] Chen and Qian used principal component analysis and shrinkage technique for de-noising this type of image. Donoho and Johnstone in [14] introduced an algorithm to de-noise hyper-spectral images in spatial domain. Lewen Dong in [10] proposed adaptive de-noising based on thresholding technique. In [15] efficiency of wavelet coefficients thresholding is introduced as a method to de-noise images. In [16] Zhang proposed cubic total variation (CTV) for hyper-spectral image de-noising. Framelet transform using normal shrinkage is proposed as well to de-noise hyper-spectral images [17]. In [18] Zhang proposed hyper spectral image de-noising based on neural network thresholding technique. In addition, Sahraeian used improved thresholding neural network to remove noise from images. In this thesis, un-decimated wavelet transform combined with improved soft thresholding is proposed to reconstruct the noisy bands in hyper-spectral images.

1.3.1 Thesis Objective

The most important purpose of a good method in image de-noising is to discard noise from image almost completely and enhance the visual resolution properly. The

objective of this thesis is to apply improved soft threshold on Un-decimated Wavelet Transform (UWT) to get reconstructed image from its noisy version. This method is proposed to decrease the presence of noise in image and improve the quality in terms of PSNR as maximum as possible.

1.3.2 Thesis Contributions

There are three main contributions in this thesis. The first one is applying Discrete Wavelet Transform (DWT) for both 2D and 3D version on image using hard and soft thresholding to observe and compare the results. The second contribution is to apply Un-decimated Wavelet Transform (UWT) for 2D and 3D versions for both hard and soft thresholding again and then compare the result of analysis to determine the best method according to the PSNR value among the methods mentioned above and finally the third contribution is to apply improved soft thresholding on that wavelet transform which has extracted from second contribution and it is expected that the combination of improved wavelet transform as proposed method with 3D-UWT gives the best quality in both the resolution and the amount of PSNR.

1.4 Thesis Overview

In chapter one, general information about hyper-spectral images and de-noising techniques has been introduced. In chapter two, 2D and 3D-DWT have been worked for both soft and hard thresholding. In chapter three, database, noise model and calculation of PSNR are discussed. Proceeding chapter is about experimental results and discussions. In addition, according to lack of translation invariance property in DWT it is preferred to use UWT as a translation invariant WT, so we worked on 2D and 3D-UWT in this chapter as well for both soft and hard thresholding techniques and finally improved soft thresholding has applied to 3D-UWT for soft thresholding

as a proposed method to increase the resolution of image and enhance the amount of PSNR. Finally, we allocated chapter five for conclusion and future work.

Chapter 2

DISCRETE WAVELET TRANSFORM FOR DE-NOISING

2.1 Introduction

Image corruption with unwanted noise is kind of common problem, so proper image analyzing and improving the quality will not be possible until we remove these noises from images [19]. The aim of de-noising is to remove noise from image to provide us with an image which is much more distinguishable and this will result in retaining most important features and characteristics of image. Hyper-spectral images are made up of spectral/spatial band. There are some corrupted bands between these spectral data, so de-noising these corrupted bands is very significant [4].

Wavelet Transform is a worldwide technique which is very useful in Chemistry, Physics, Applied Science and Engineering. In signal and image processing, it is an appropriate method in de-noising, signal and image analysis and data compression. During acquisition and transition process, an image can be contaminated by noise [20]. Discrete Wavelet Transform (DWT) has become a popular method in terms of image de-noising recently to distinguish image from its noisy version. This wavelet transform can also be joined with thresholding to work on wavelet coefficients before reconstruction process [19].

2.2 Discrete Wavelet Transform

Foundation of DWT goes back to 1976 while Croiser, Esteban and Galand were working on a technique to decompose discrete time signal. Their work followed by some unique innovation like sub-band coding and pyramidal coding which is famous as multi-resolution analysis. Discrete wavelet transform is not translation invariant. It means that, translated version and original signal is not same in DWT. This wavelet transform, provide adequate information for analyzing and synthesis original image in a short time [21].

In Figure 2.1 a general block diagram of DWT is given. In this diagram, an original signal x can pass among a half band low pass filter with impulse response g. This signal also pass through half band high pass filter h. This decomposing results in detail and approximation coefficients (2.1). Passing signal among low pass filter, provides us with discarding all high frequencies.

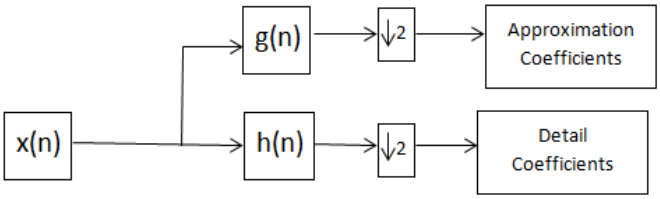

Figure 2.1: Block Diagram of Low Pass and High Pass Filter Analysis [21].

$$g(n) = (x * g)(n) = \sum_{k=-\infty}^{\infty} x(k)g(n-k) \qquad (2.1)$$

Figure 2.2 shows three level of decomposition for DWT. In this figure, when signal passed the half band low pass filter, we remove other half sample based on Nyquist's rule. Whenever we want every half to be removed, the signal will be subsampled by 2. It means that, subsampling will double the scale but low pass filtering does not

change the scale. By filtering (low pass filter), half of the frequencies will be discarded, so we do not have half of the information. To make it clear, the resolution will be halved after doing low pass filter (level one). According to what is said above, the resolution and scale are dependent to filtering and up-sampling, respectively.

To continue the process, in level two, the output of the low pass filter $g(n)$ shown in Figure 2.1 which has subsampled by 2 will pass among high pass and low pass filter again with half of the previous cutoff frequencies [21]. In level three, we will have the same process as we saw in level one and two. In this wavelet transform, coefficients (approximation and details) will be down-sampled at each level.

$$g(n) = \sum_{k=-\infty}^{\infty} x(k)g(2n-k) \tag{2.2}$$

$$h(n) = \sum_{k=-\infty}^{\infty} x(k)h(2n-k) \tag{2.3}$$

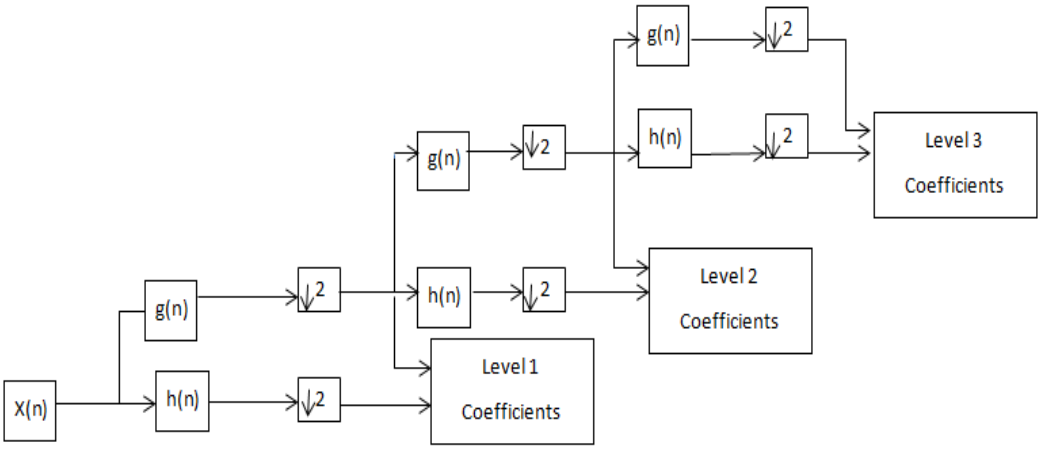

Figure 2.2: Three Level of Decomposition for DWT [22].

2.2.1 2D-Discrete Wavelet Transform

Figure below shows 2D-DWT for one level of decomposition which is result of applying 1D-DWT on both rows and columns. As a result, we will get four sub images which three of them contain high frequencies called HH, LH and HL and one of them contains low frequency called LL.

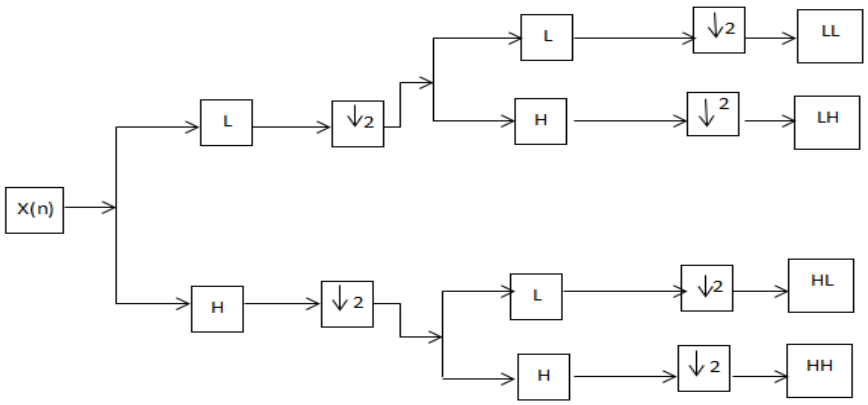

Figure 2.3: First Level Decomposition for 2D Discrete Wavelet Transform [23].

2D-DWT allows an image to cross among low pass and high pass filter. Figure 2.4 shows the process of three level of decomposition for 2D-DWT. It is clear that the higher level of decompositions take place in LL sub-band. In Figure 2.4 (a) we see one level of decomposition for 2D-DWT, in (b) we see two level of decomposition for 2D-DWT and in (c) we see three level of decomposition for 2D-DWT.

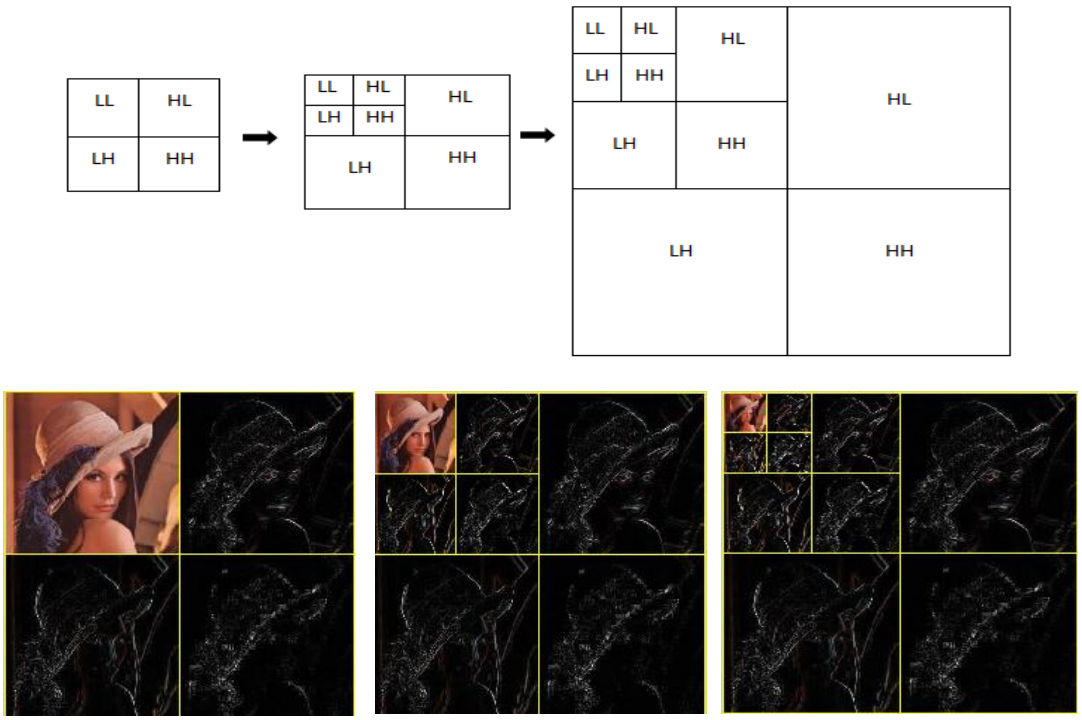

(a) (b) (c)

Figure 2.4: (a) One, (b) Two and (c) Three Level of Decomposition for 2D-DWT [22], [24].

2.2.2 3D-Discrete Wavelet Transform

3D-DWT is result of applying 1D-DWT on x (rows), y (columns) and z (spectral) directions. This wavelet transform will give 8 sub-images called LLL,LLH,LHL,LHH,HLL,HLH,HHL,HHH which is shown in Figure 2.5. In addition, higher level of decomposition will be processed in LLL as shown in Figure 2.6. In this figure, in level one we see eight sub images as mentioned above and for the next levels, these eight sub images will be produced just in LLL sub image.

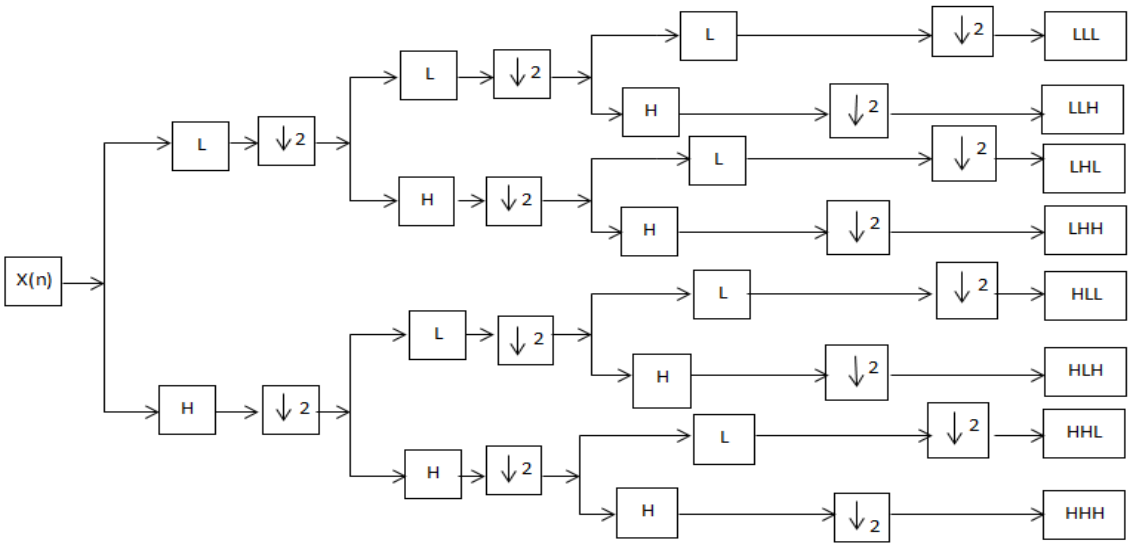

Figure 2.5: First Level of Decomposition for 3D-DWT [25].

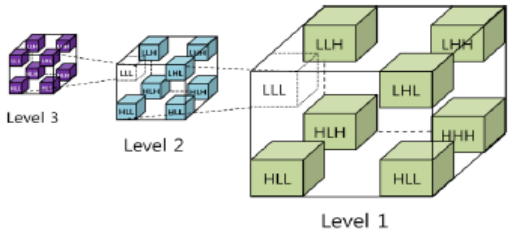

Figure 2.6: The Process of Three Level Decomposition of 3D-DWT [24].

2.3 Choice of Threshold

Here $\{f(x,y),\ 1 < (x,y) < n\}$ is our original image with size N=n× n and this image can be influenced by White Gaussian Additive Noise which the noisy model is as the following:

$$g(x,y) = f(x,y) + \eta(x,y) \qquad 1 < (x,y) < n \qquad (2.4)$$

where $\eta(x,y)$ is AWGN with zero mean and standard deviation of σ. Our aim is to recover $f(x,y)$ by discarding noise from $g(x,y)$ under this condition that Peak Signal to Noise Ratio will be as maximum as possible.

In (2.4) wavelet coefficient for $g(x,y)$ is y_{jk}which j is decomposition level and k is the index of the coefficients in this level. In wavelet domain it can be written as the following:

$$y_{jk}=\omega_{jk}+e_{jk} \tag{2.5}$$

where ω_{jk} is the coefficients of $f(x,y)$ which includes detail coefficients dc_{jk} and approximation coefficients ac_{jk}. In addition, e_{jk} is $N(0,\sigma^2)$.

Donoho suggested an estimator as following which is useful in finding estimated noise deviation by a robust median estimator of the highest sub-band diagonal coefficients (median absolute deviation) HH or HHH[16].

$$\sigma_n = Median\,(\,|Y_{x,y}|\,)/0.6745\,,\quad Y_{x,y} \in Subband\ HH \tag{2.6}$$

Then universal threshold value is as the following:

$$T = \sigma_n \sqrt{2log(n)} \tag{2.7}$$

where $Y_{x,y}$ is wavelet detail coefficient in diagonal direction [15] and σ_n is the standard deviation of the noise from the sub-band HH or HHH which is the result of distribution of dc_{jk} as detail coefficient and the scale part as denominator which is equal to 0.6745. Besides, n is the sample size.

Here for 2D wavelet transform, $Y_{x,y}$is wavelet coefficient for sub-band HH and for 3D wavelet transform, $Y_{x,y}$is wavelet coefficient for sub-band HHH [4]. This threshold is known as universal or global thresholding. After choosing the threshold value, we can apply hard or soft thresholding to work on wavelet coefficients which

results in getting wavelet thresholded coefficients. Finally, we can obtain the de-noised image by applying IDWT.

2.4 Wavelet Thresholding Techniques

2.4.1 Hard Threshold

With hard thresholding technique, wavelet coefficients, ω, which their absolute value stays below threshold value,T, will be zero (killed) and wavelet coefficients larger than , T, will be kept. [10], [15].

$$P_H(\omega) = \begin{cases} \omega\,, & |\omega| > T \\ 0\,, & otherwise \end{cases} \tag{2.8}$$

Figure 2.7 shows Hard thresholding function where x-direction is , ω, values which are wavelet coefficients and y-direxction is $P_H(\omega)$ as threshold function.

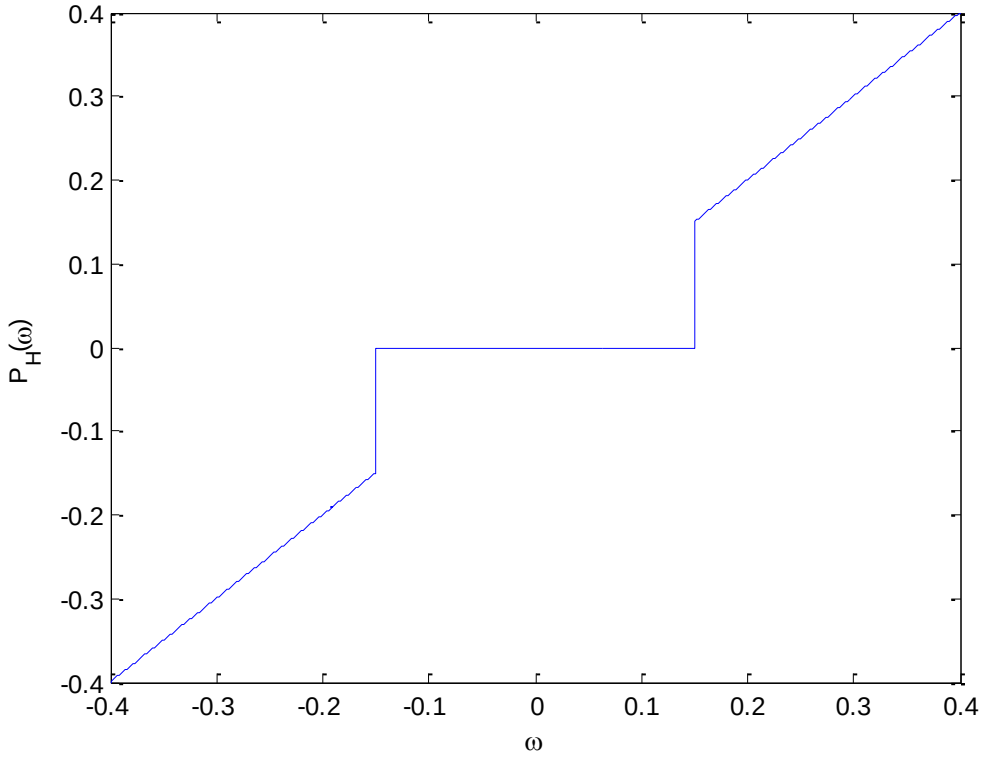

Figure 2.7: Hard Thresholding Function.

2.4.2 Soft Threshold

With hard thresholding technique, wavelet coefficients , ω, which their absolute value stays below threshold value , T, will be shrunk by , T, [10], [15] and wavelet coefficients larger than , T, will be kept.

$$P_S(\omega) = \begin{cases} sgn(\omega).(|\omega| - T), & |\omega| \geq T \\ 0 \quad , & |\omega| < T \end{cases} \tag{2.9}$$

In Figure 2.8 we see Soft thresholding function where x-direction is ω values which are called wavelet coefficients and y-direxction is $P_S(\omega)$ as threshold function.

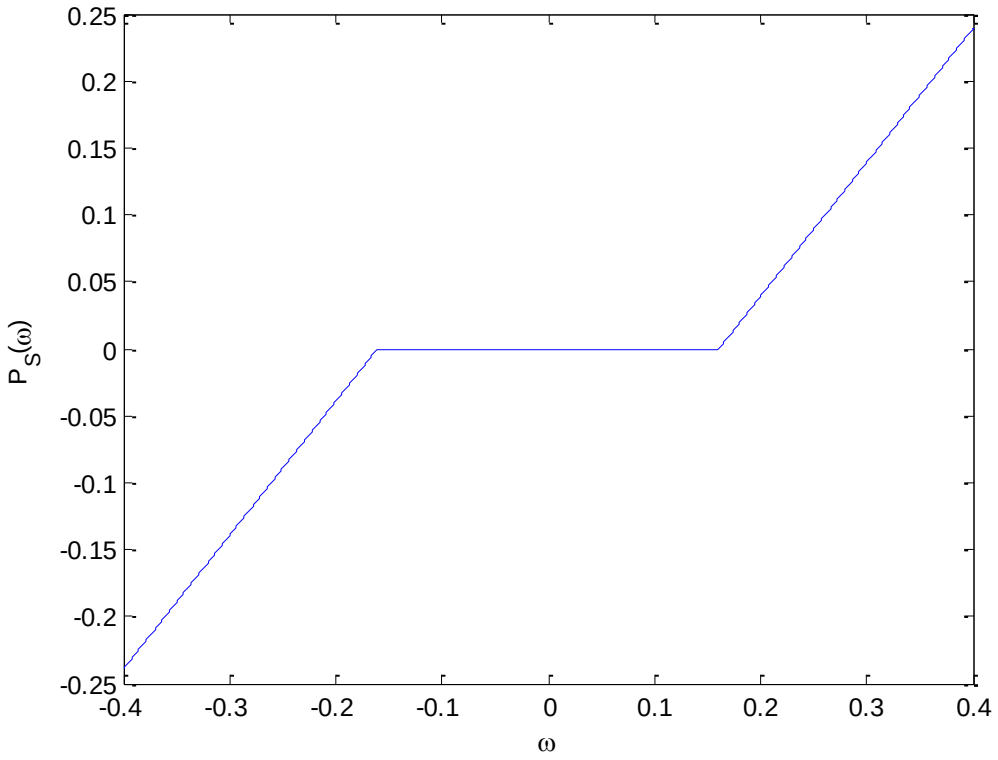

Figure 2.8: Soft Thresholding Function.

Hard thresholding is called ‘’keep or kill’’ process while soft thresholding is known as ‘’keep or shrink’’ process [26]. Hard thresholding is discontinuous while soft is continuous, so soft thresholding performs better than hard because the number of elements in soft thresholding are more than hard. It is clear that when we have more

elements, we can characterize a picture better based on their main features. On the other hand, hard thresholding keeps edges better rather than soft [9].

2.5 Image De-noising

Our aim is to get a de-noised or reconstructed image from its noisy version by removing small noisy coefficients which is required to threshold wavelet coefficients. Applying DWT on our image is followed by transforming data from time to time-frequency domain. These transformed data values are called coefficients, so by DWT we will be able to compute wavelet coefficients, moreover; these coefficients can be categorized in two types: one is crucial wavelet coefficients carrying the most important character or information of image and other is non-important wavelet coefficients called noisy coefficients. Based on Donoho's idea, we can repress noise by selecting a proper threshold value [27]. Proceeding step is setting a threshold value to see which coefficients can cross this value. A plus point is that some coefficients cannot go further than this threshold value and some of them can be shrunk by this value which is because of applying hard and soft thresholding, respectively. The last step is applying inverse discrete wavelet transform to reconstruct the image from thresholded wavelet coefficients [15], [26]. Figure 2.9 shows a general Block Diagram of De-noising process. It starts with input noisy image which DWT should be applied on it and then we should choose threshold value. After choosing threshold value, we should apply hard or soft thresholding functions to acquire thresholded wavelet coefficients. Proceeding step is applying the Inverse Discrete Wavelet Transform (IDWT) to get reconstructed or de-noised image.

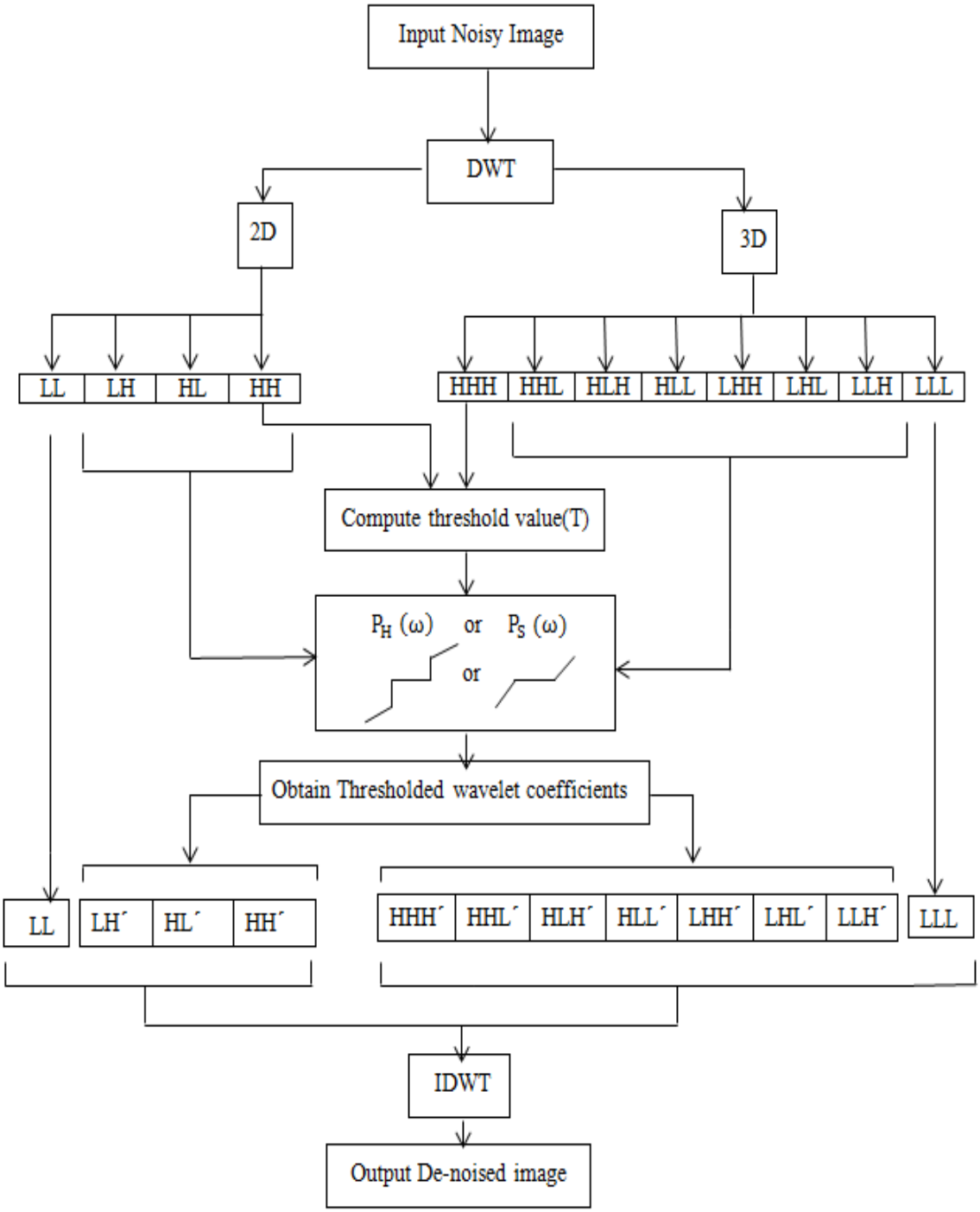

Figure 2.9: General Block Diagram of Proposed De-noising Process.

2.6 Performance Analysis Based on DWT Using Hard and Soft Thresholding

In the first experiment, Indian pine hyper-spectral image is used to analyze de-noising procedure for hard and soft thresholding technique which is shown in figure

2.10. Our original image is band 25 of Indian Pine data set and we apply White Gaussian Additive Noise with zero mean and standard deviation of 20 to obtain a noisy image.

In figure 2.10, (a) is the original band 25 of Indian Pine, (b) is noisy image with PSNR of 21.98dB, (c) is de-noised image based on 2D-DWT using hard thresholding with PSNR of 26.29dB and (d) is de-noised image based on 3D-DWT using hard thresholding with PSNR of 27.98dB. Here after applying de-noising process we found out 3D-DWT performs better than its 2D version in terms of PSNR.

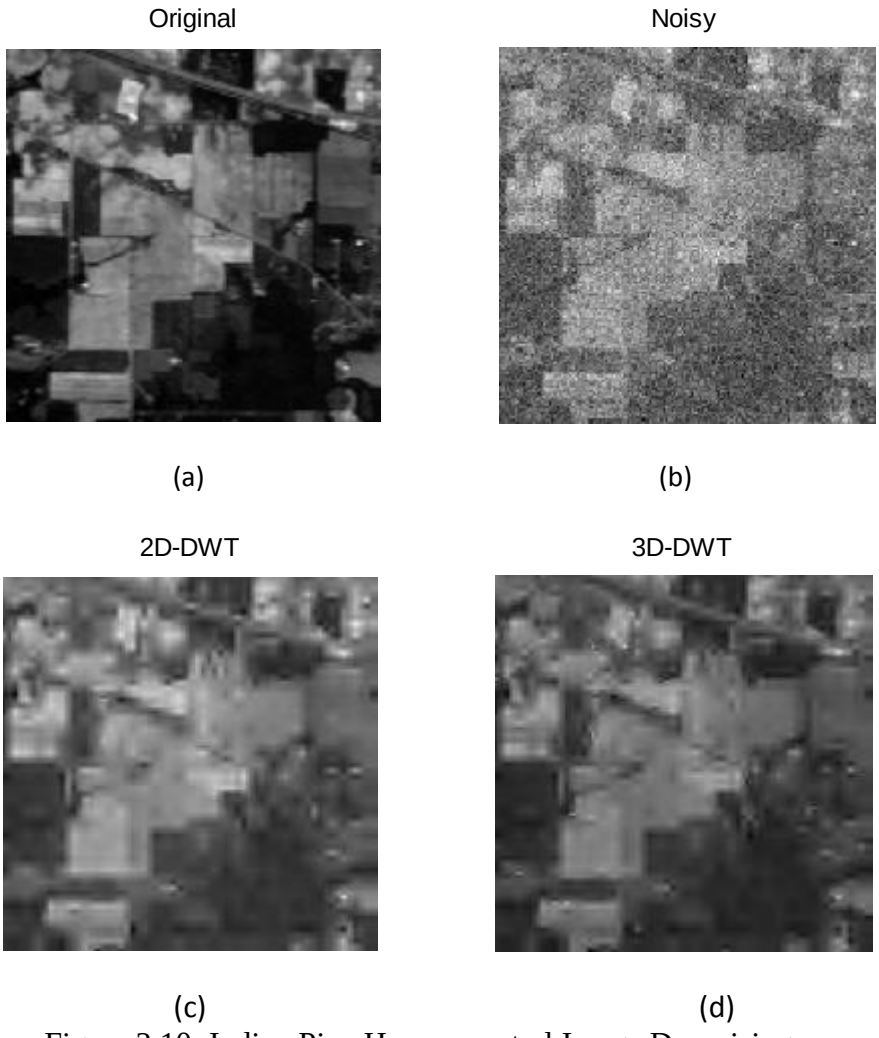

Figure 2.10: Indian Pine Hyper-spectral Image De-noising Based on DWT with Hard Thresholding Technique.

Figure 2.11 Shows Indian Pine hyper-spectral image de-noising based on soft thresholding technique for 2D-DWT and 3D-DWT [4]. In Figure 2.11(a) is the original band 25 of Indian Pine, (b) is noisy image with PSNR of 21.98dB, (c) shows the de-noised image based on 2D-DWT with soft thresholding method and PSNR is equal to 27.32 dB and in (d) we can see the de-noised image based on 3D-DWT using soft thresholding technique and PSNR value is equal to 28.78 dB, so here 3D-DWT outperforms the 2D one because of the higher PSNR value.

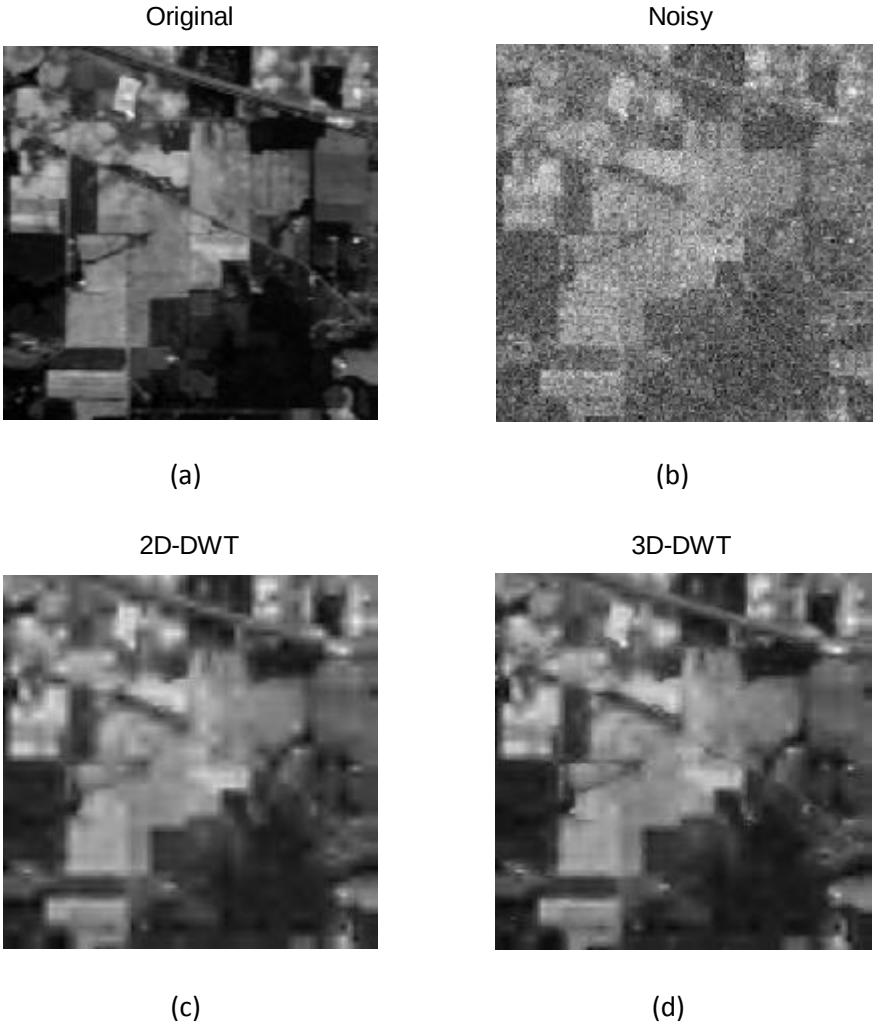

Figure 2.11: Indian Pine Hyper-spectral Image De-noising Based on DWT with Soft Thresholding Technique.

In the second experiment Gulf of Mexico hyper-spectral image is used to process image de-noising based on 2D and 3D-DWT using hard and soft thresholding. Figure 2.12 shows de-noising based on DWT using hard thresholding technique for Gulf of Mexico. Here (a) is original image, (b) noisy image with PSNR value of 20.45 dB, (c) is de-noised image based on 2D-DWT using hard thresholding with PSNR of 26.10dB and (d) is de-noised image based on 3D-DWT using hard thresholding with PSNR of 28.02 dB. In this figure, (d) performs better rather than (c) in terms of resolution and PSNR value.

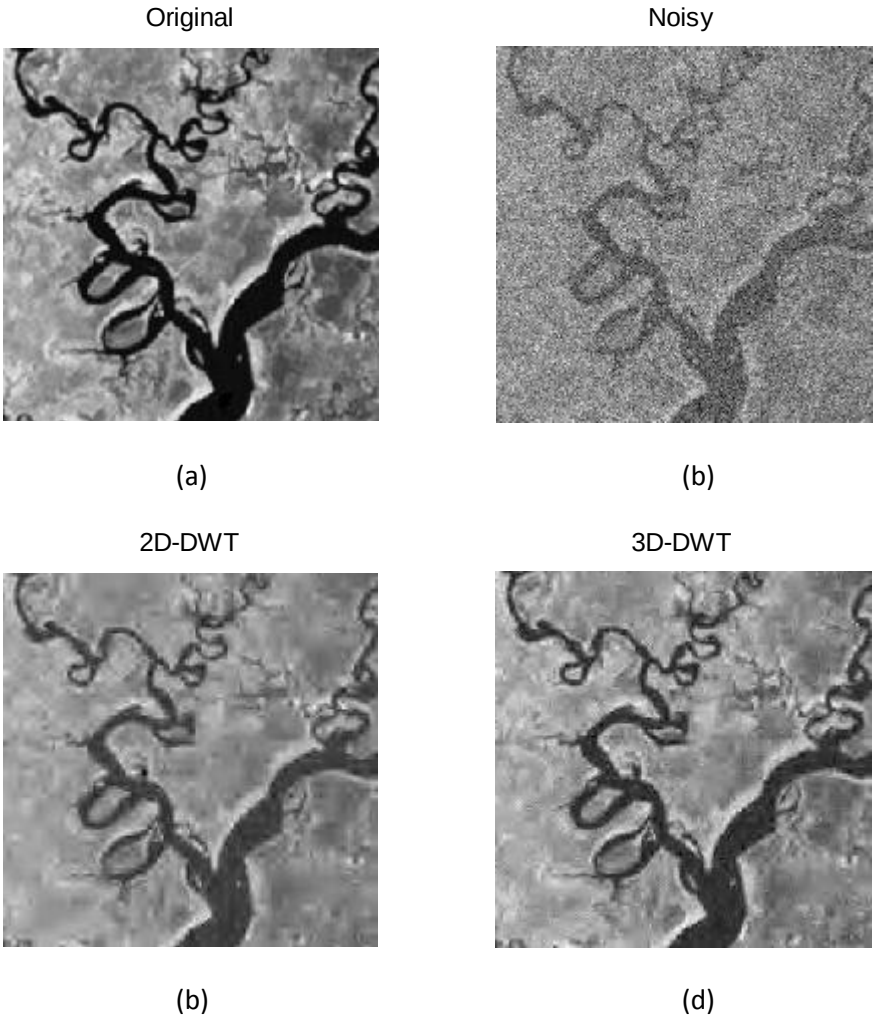

Figure 2.12: Gulf of Mexico Hyper-spectral Image De-noising Based on DWT with Hard Thresholding Technique.

In Figure 2.13 we can see de-noising based on 2D and 3D-DWT using soft thresholding technique for Gulf image. Here (a) is original image, (b) noisy image with PSNR value of 20.45 dB, (c) is de-noised image based on 2D-DWT using soft thresholding with PSNR of 27.36dB and (d) is de-noised image based on 3D-DWT using soft thresholding with PSNR of 28.83 dB. In this figure, (d) is better than (c) because of its performance in obtaining higher PSNR value and resolution.

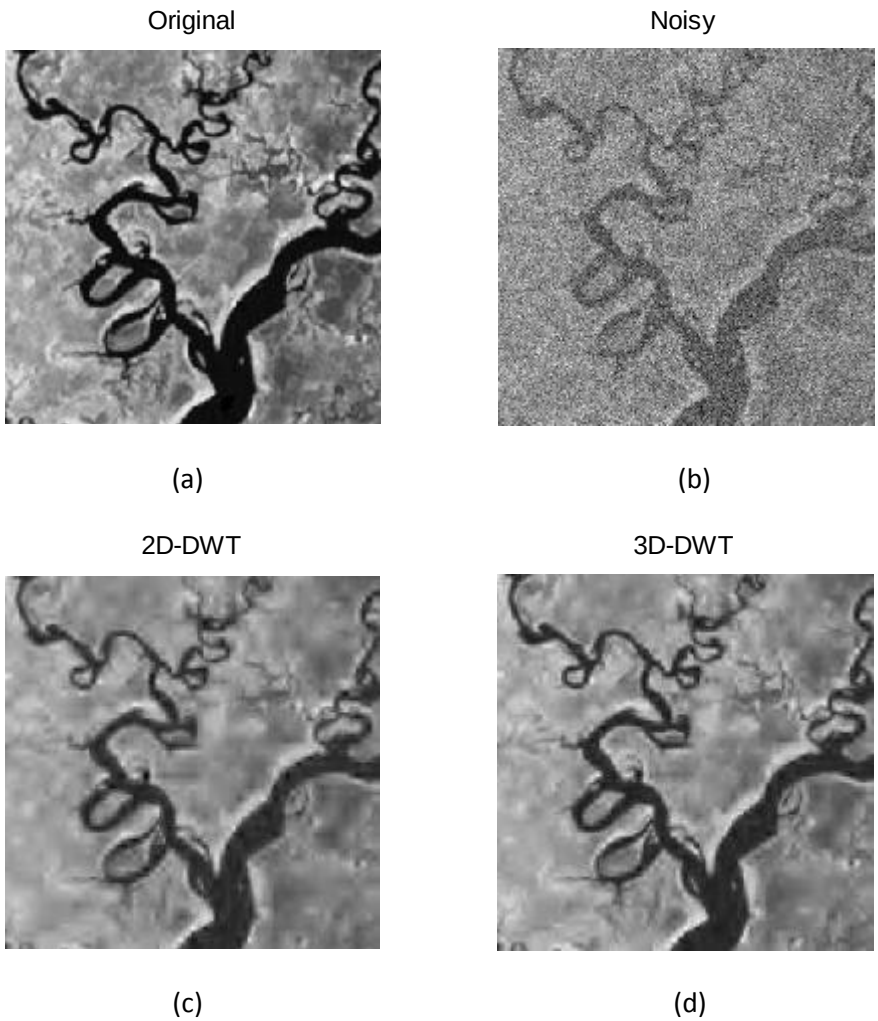

Figure 2.13: Gulf of Mexico Hyper-spectral Image De-noising Based on DWT with Soft Thresholding Technique.

In the third experiment, in several tables and graphs the performance of hyper-spectral image de-noising based on DWT using hard and soft thresholding has discussed. In this experiment, Indian Pine data set has used to work on de-noising procedure. Table 2.1 shows analysis of 2D-DWT and 3D-DWT based on hard thresholding technique for band 25, average of 10 experiments of band 25, average of all bands and average of 8 specific bands.

Table 2.1: The Result of De-noising the Indian Pine Hyper-spectral Image Using Hard Threshold.

PSNR(dB)	Additive Gaussian Noise (σ=20,zero mean)	2D-DWT	3D-DWT
		Hard Thresholding	Hard Thresholding
Indian Pine for band 25	21.98	26.29	27.98
Average of 10 experiments	21.83	26.22	27.91
Average of all bands	22.02	26.10	27.11
Average of bands(20-28)	22.10	26.15	27.43

In Figure 2.14 we see the analysis extracted from (Table 2.1) in a graph where x-direction represents the number of bands and y-direction denotes PSNR value. In this figure, we see PSNR vs Band for noisy image, de-noised with 2D-DWT and 3D-DWT based on hard thresholding.

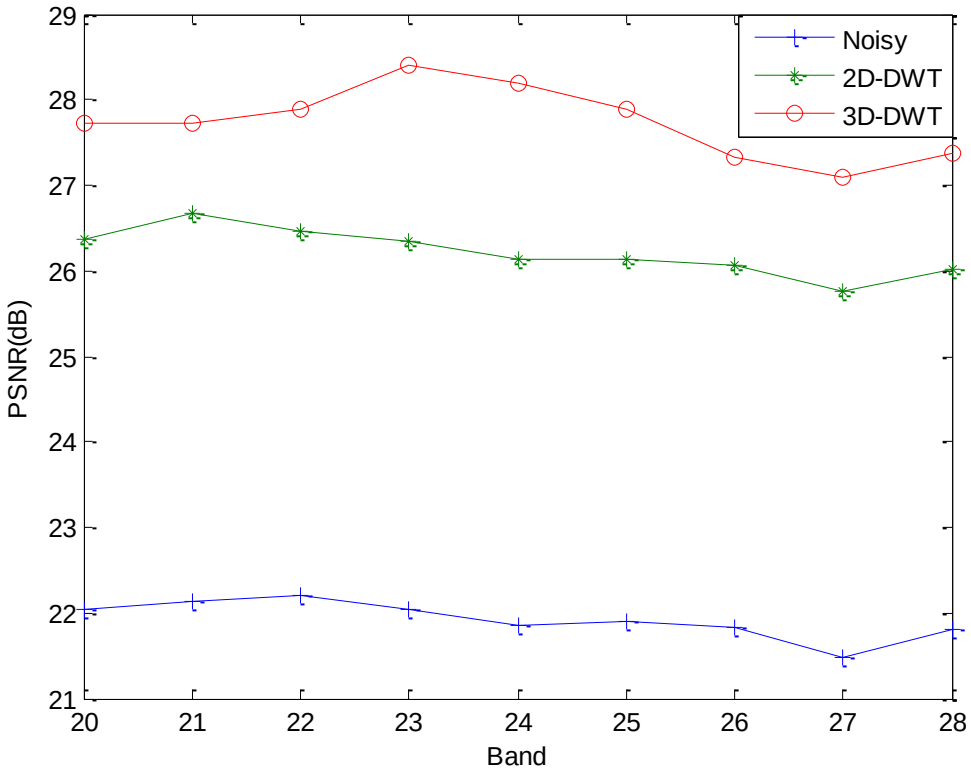

Figure 2.14: The PSNR Values vs Band for the Indian Pine Hyper-spectral Image (bands 20-28) for Hard Thresholding.

Table 2.2 shows analysis of 2D-DWT and 3D-DWT based on soft thresholding technique for band 25, average of 10 experiments of band 25, average of all bands and average of 8 specific bands.

Table 2.2: The Result of De-noising the Indian Pine Hyper-spectral Image Using Soft Threshold

PSNR(dB)	Additive Gaussian Noise (σ=20,zero mean)	2D-DWT	3D-DWT
		Soft Thresholding	Soft Thresholding
Indian Pine for band 25	21.98	27.32	28.78
Average of 10 experiments	21.83	27.26	28.84
Average of all bands	22.02	27.14	28.21
Average of bands(20-28)	22.10	27.31	28.39

In Figure 2.15 we see the analysis extracted from (Table 2.2) in a graph where x-direction represents the number of bands and y-direction denotes PSNR value. This figure shows PSNR vs Band for noisy image, de-noised image with 2D-DWT and 3D-DWT based on soft thresholding.

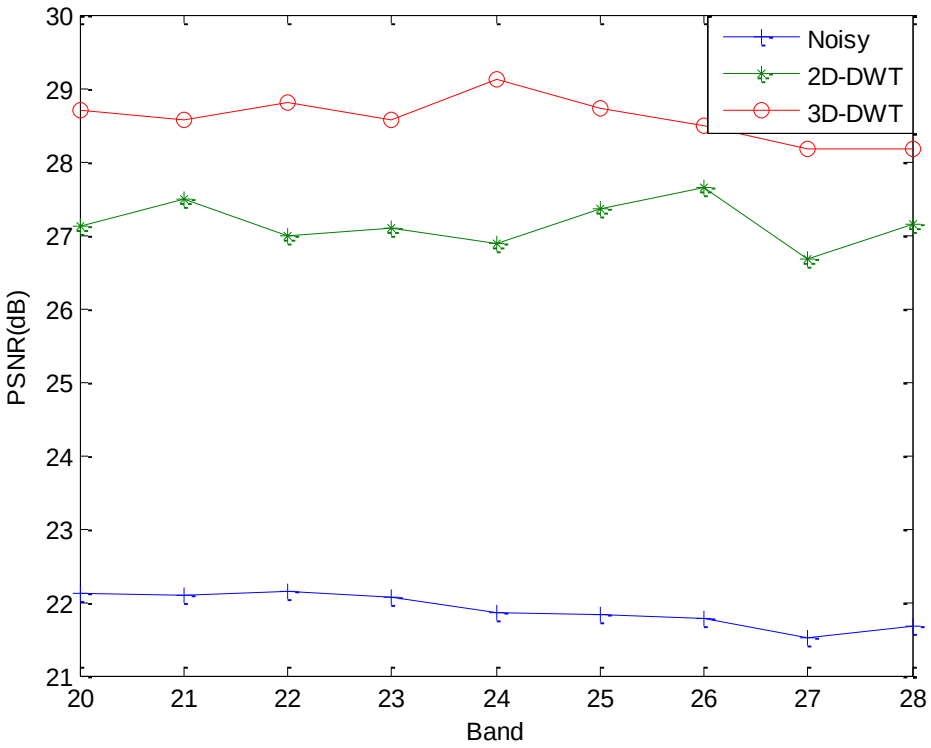

Figure 2.15: The PSNR Values vs Band for the Indian Pine Hyper-spectral Image (bands 20-28) for Soft Thresholding.

In the fourth experiment, the analysis of de-noising based on DWT has performed. In this experiment we see several tables and graphs. In addition, in these tables the de-noising process has applied on Washington DC Mall data set. Here hard and soft thresholding techniques have been used in de-noising with DWT. Table 2.3 shows analysis of 2D-DWT and 3D-DWT based on soft thresholding technique for band 25, average of 10 experiments for band 25, average of all bands and average of 8 specific bands of WDM data set. In addition, Table 4 shows these results using soft thresholding.

Table 2.3: The Result of De-noising the Washington DC Mall Hyper-spectral Image Based on 2D and 3D-DWT Using Hard Thresholding.

PSNR(dB)	Additive Gaussian Noise (σ=20,zero mean)	2D-DWT	3D-DWT
		Hard Thresholding	Hard Thresholding
WDM for band 25	22.48	28.10	28.32
Average of 10 experiments	22.25	27.98	28.23
Average of all band	22.16	27.65	28.48
Average of 8 bands(20-28)	22.27	27.87	28.82

Figure 2.16 shows the performance analysis from (Table 2.3) in a graph where x-direction represents the number of bands and y-direction denotes PSNR value. In this figure, we see PSNR vs Band for noisy image, de-noised with 2D-DWT and 3D-DWT based on hard thresholding.

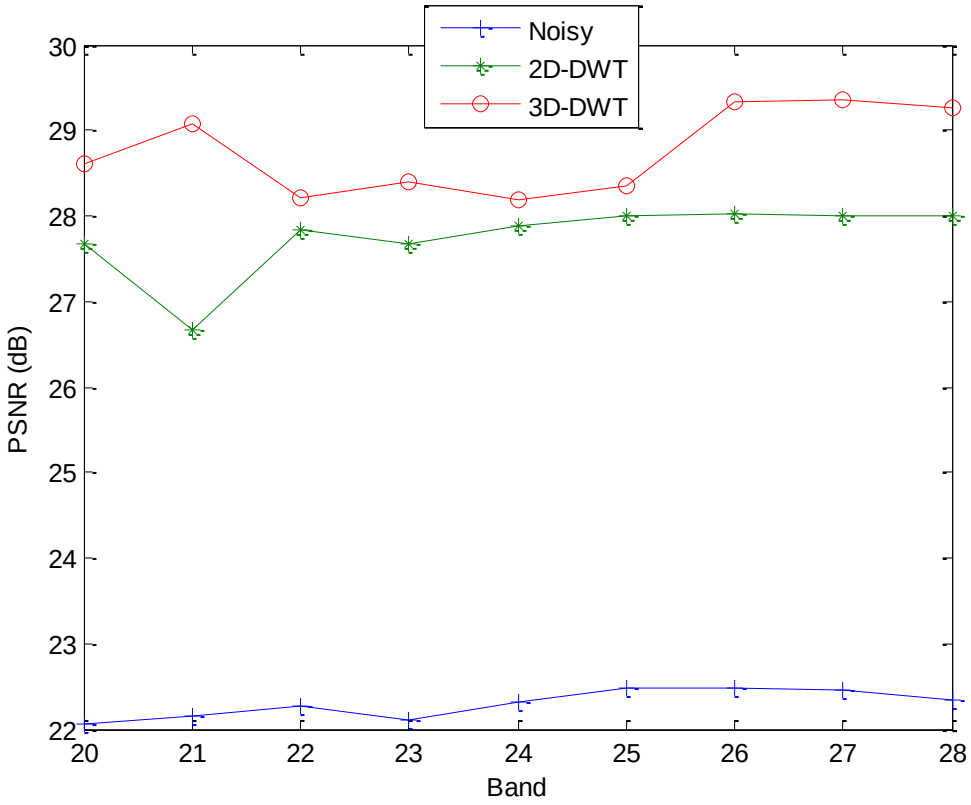

Figure 2.16: The PSNR Values vs Band for the WDM Hyper-spectral Image (bands 20-28) for Hard Thresholding.

Table 2.4: The Result of De-noising the WDM Hyper-spectral Images Based on 2D and 3D-DWT Using Soft Threshold.

PSNR(dB)	Additive Gaussian Noise (σ=20,zero mean)	2D-DWT	3D-DWT
		Soft Thresholding	Soft Thresholding
WDM for band 25	22.48	28.71	29.41
Average of 10 experiments	22.25	28.58	29.22
Average of all band	22.16	27.65	28.48
Average of 8 bands(20-28)	22.27	28.12	30.21

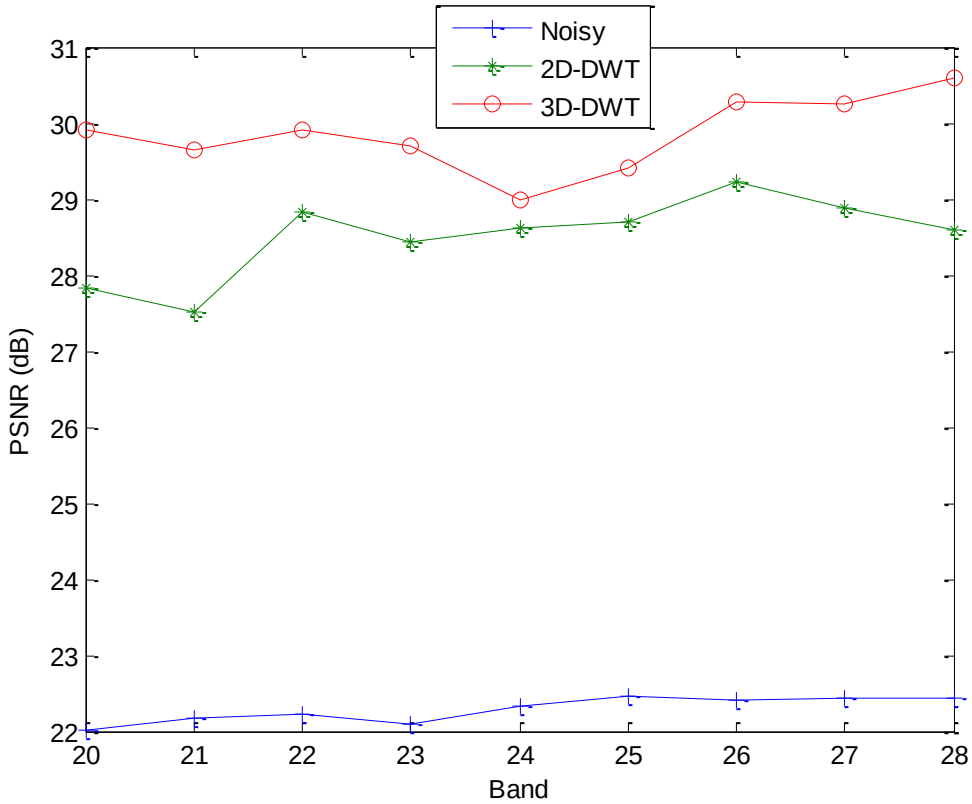

Figure 2.17: The PSNR Values vs Band for the WDM Hyper-spectral Image (bands 20-28) for Soft Thresholding.

In Figure 2.17 we can see the analysis extracted from (Table 2.4) in a graph where x-direction represents the number of bands and y-direction denotes PSNR value. This

figure shows PSNR vs Band for noisy image, de-noised image with 2D-DWT and 3D-DWT based on soft thresholding.

According to tables and figures above, in our first experiment, de-noising for 2D and 3D Discrete Wavelet Transform based on Hard Thresholding technique discussed and in proceeding experiment, the same process has done for Soft Thresholding technique and we found out 3D version was better than 2D one in terms of PSNR in both hard and soft thresholding techniques. A plus point is that, de-noising with soft thresholding outperforms hard thresholding according to visual inspection and PSNR value. It is clear that the average of PSNR for all bands of Indian Pine for 3D-DWT using soft thresholding is 28.21 (dB) and for hard thresholding is 27.11 (dB). In this way, there is a 1.10 dB difference between soft and hard thresholding techniques. To sum up, our best result till now is for 3D-DWT using soft thresholding method.

Chapter 3

METHODOLOGY

3.1 Dataset Used

In this thesis we used different kinds of hyper-spectral data sets during the de-noising process in tables, graphs and figures. Indian Pine hyper-spectral data set is assembled by AVIRIS sensor taken from north-western Indiana City, US. The original data set include 145× 145 in 224 bands. Figure 3.1 shows Indian Pine hyper-spectral image.

Second data set used in this thesis was Washington DC Mall which consists 210 bands in the range of 0.4-2.4μm. This data set contains 1208 scan line with 307 pixels among each scan line. These two data sets are available at Purdue's University Multi-Spec Site. Figure 3.2 shows WDM hyper-spectral image.

Pavia Center and University have also used in this thesis. These data sets have obtained by ROSIS sensor and taken over Pavia which is located in the north part of Italy. Pavia Center and University are 1096×1096 and 610×610 pixels, respectively. In addition, Pavia Center contains 102 and Pavia University includes 103 spectral bands. Figure 3.3 and Figure 3.4 show Pavia Center and Pavia University.

Gulf of Mexico Wetland Sample is another data set used in this thesis which is taken from Spec TIR's extensive data sets over Gulf of Mexico. This data set gathered at a 2m Spatial resolution, 5nm band spacing covering the spectral range of 395-

2450nm(Figure 3.5). US Government photograph of Arizona Mining is also used in this thesis which is gathered with hyper-spectral imaging (Figure 3.6).

Another data set which is used in this thesis is Cuprite Mining District, Nevada obtained by AVIRIS. The original size is 614×512 in 224 bands. Figure 3.7 shows cuprite hyper-spectral image.

Table 3.1 shows the wavelengths for hyper-spectral bands. In this table in each column, the left numbers are the number of bands and right numbers are centeral wavelengths in μm. Here we have 210 bands and for each band we have one wavelength with bandwidth of $2\mu m$.

Table 3.1: Wavelength (μm) for hyper-spectral bands of WDM.

Band	Central Wavelength (μm)	Band	Central Wavelength (μm)	Band	Central Wavelength (μm)
1	401.288	41	586.411	81	1040.51
2	404.590	42	593.518	82	1055.31
3	407.919	43	600.815	83	1070.16
4	411.279	44	608.309	84	1085.06
5	414.671	45	616.006	85	1099.97
6	418.100	46	623.912	86	1114.90
7	421.568	47	632.031	87	1129.85
8	425.078	48	640.368	88	1144.79
9	428.632	49	648.930	89	1159.73
10	432.235	50	657.721	90	1174.65
11	435.888	51	666.745	91	1189.55
12	439.595	52	676.005	92	1204.42
13	443.358	53	685.506	93	1219.26
14	447.182	54	695.249	94	1234.06
15	451.067	55	705.237	95	1248.82
16	455.019	56	715.473	96	1263.53
17	459.040	57	725.956	97	1278.19
18	463.134	58	736.686	98	1292.78
19	467.302	59	747.664	99	1307.32
20	471.550	60	758.887	100	1321.80
21	475.880	61	770.353	101	1336.21
22	480.298	62	782.060	102	1350.55
23	484.805	63	794.003	103	1364.81
24	489.406	64	806.177	104	1379.01
25	494.105	65	818.576	105	1393.13
26	498.906	66	831.195	106	1407.18
27	503.814	67	844.025	107	1421.14
28	508.832	68	857.059	108	1435.03
29	513.966	69	870.287	109	1448.84
30	519.221	70	883.702	110	1462.57
31	524.600	71	897.292	111	1476.21
32	530.109	72	911.048	112	1489.78
33	535.752	73	924.959	113	1503.26
34	541.537	74	939.015	114	1516.67
35	547.467	75	953.203	115	1529.99
36	553.547	76	967.514	116	1543.22
37	559.784	77	981.935	117	1556.38
38	566.183	78	996.454	118	1569.46
39	572.751	79	1011.06	119	1582.44
40	579.491	80	1025.75	120	1595.35

Band	Central Wavelength (μm)	Band	Central Wavelength (μm)	Band	Central Wavelength (μm)
121	1608.19	161	2062.64	201	2431.42
122	1620.93	162	2072.74	202	2439.84
123	1633.61	163	2082.79	203	2448.22
124	1646.20	164	2092.79	204	2456.57
125	1658.70	165	2102.74	205	2464.88
126	1671.14	166	2112.64	206	2473.16
127	1683.49	167	2122.49	207	2481.41
128	1695.77	168	2132.29	208	2489.63
129	1707.97	169	2142.04	209	2497.81
130	1720.10	170	2151.74	210	2505.97
131	1732.15	171	2161.40		
132	1744.12	172	2171.00		
133	1756.03	173	2180.57		
134	1767.86	174	2190.08		
135	1779.62	175	2199.55		
136	1791.31	176	2208.98		
137	1802.93	177	2218.36		
138	1814.48	178	2227.70		
139	1825.96	179	2237.00		
140	1837.37	180	2246.26		
141	1848.71	181	2255.47		
142	1859.99	182	2264.63		
143	1871.21	183	2273.76		
144	1882.35	184	2282.84		
145	1893.44	185	2291.89		
146	1904.46	186	2300.90		
147	1915.42	187	2309.86		
148	1926.31	188	2318.79		
149	1937.15	189	2327.67		
150	1947.92	190	2336.53		
151	1958.64	191	2345.34		
152	1969.29	192	2354.11		
153	1979.89	193	2362.84		
154	1990.43	194	2371.54		
155	2000.91	195	2380.21		
156	2011.34	196	2388.83		
157	2021.71	197	2397.42		
158	2032.02	198	2405.97		
159	2042.28	199	2414.49		
160	2052.49	200	2422.98		

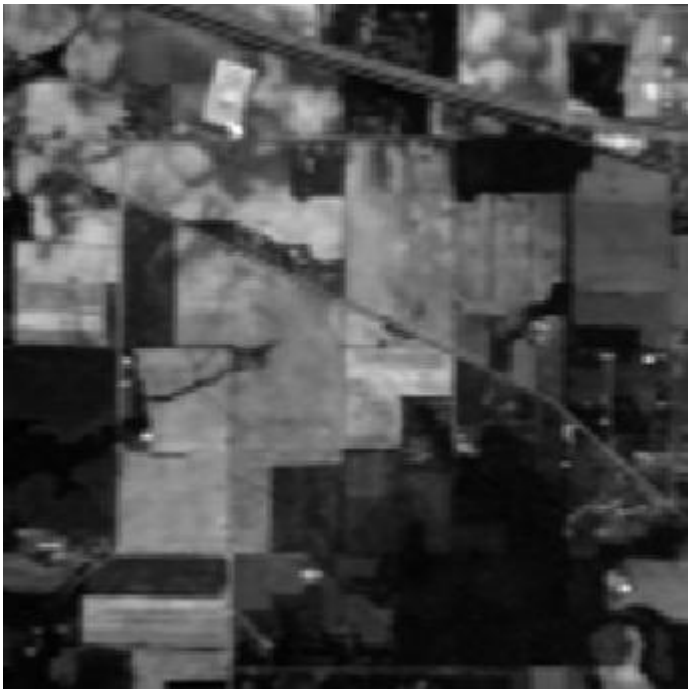

Figure 3.1: Original Indian Pine Hyper-spectral Image [4].

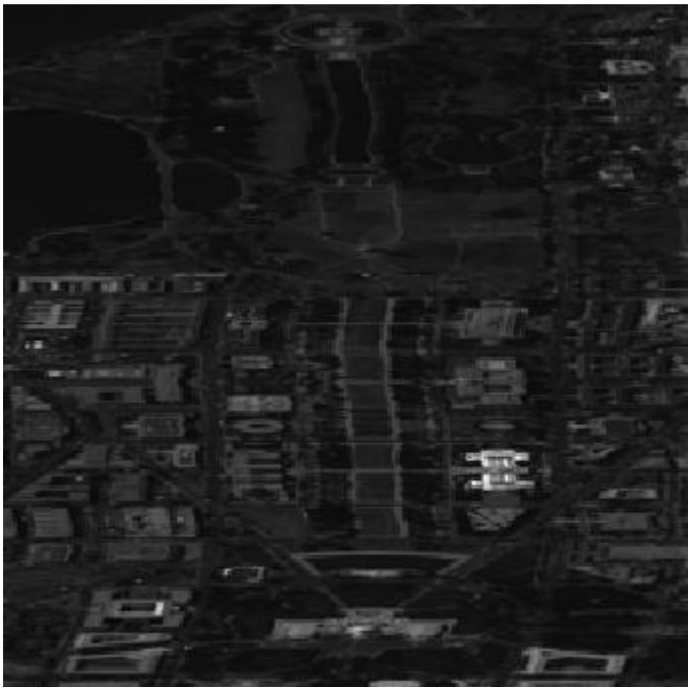

Figure 3.2: WDM Hyper-spectral Image [16].

Figure 3.3: Pavia Center Hyper-spectral Image[4].

Figure 3.4: Pavia University Hyper-spectral Image[4].

Figure 3.5: Gulf of Mexico Hyper-spectral Image [28].

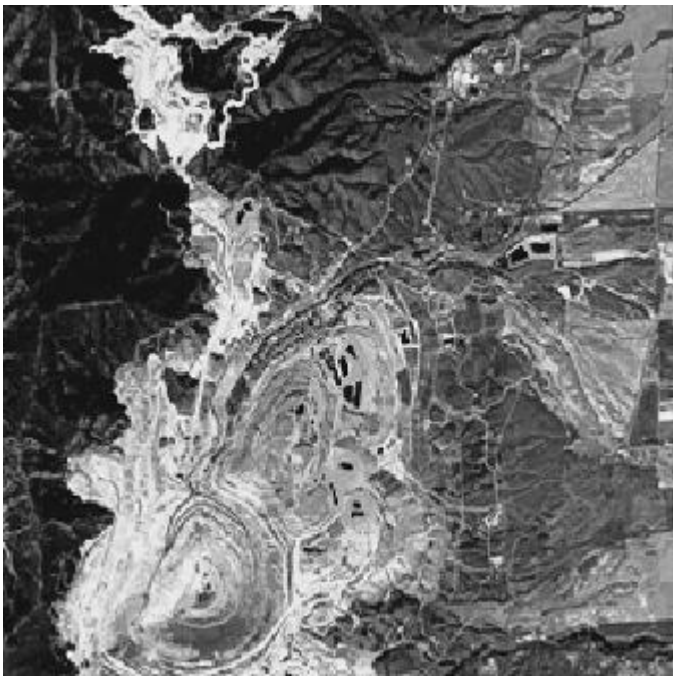

Figure 3.6: Arizona Mining Hyper-spectral Image [29].

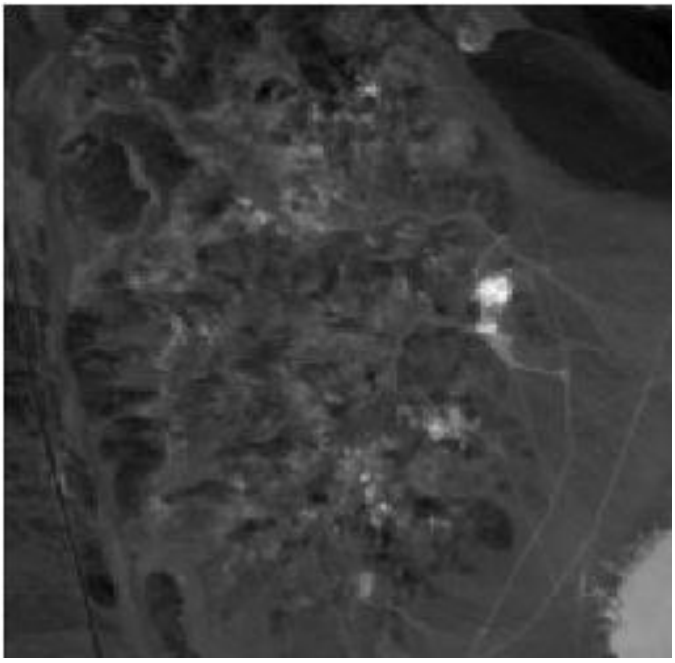

Figure 3.7: Cuprite's District Mining Hyper-spectral Image [17].

3.2 Noise Model Used

In this thesis Additive White Gaussian Noise with zero mean and standard deviation of 20 is used which we can see in the following formula

$$g(x,y) = f(x,y) + \eta(x,y) \quad 1 < (x,y) < n \tag{1.2}$$

where $\eta(x,y) \sim N(0, \sigma^2)$ is Additive White Gaussian Noise (AWGN) with zero mean and variance σ^2. Here in this thesis, AWGN is used with zero mean and standard deviation of 20.

3.3 Calculating the Quality (PSNR) of De-noised Image

According to the above formula, our goal is to remove noise from noisy image $g(x,y)$ and estimate $\hat{f}(x,y)$ under this condition that our PSNR value will be as maximum as possible. In this way, to calculate the quality of de-noised data, Peak Signal to Noise Ratio (PANR) in dB is a common method to use. Here logarithmic decibel scale is used in this method as the following:

$$\text{PSNR}=10\log_{10}\left(\frac{MAX_f^2}{MSE}\right) \tag{3.1}$$

where MAX_f is the maximum pixel value of our image which here for 8 bit per sample it is equal to 255. In addition, MSE is the squared error between original and noisy or corrupted image which is represented as the following formula:

$$\text{MSE}=\frac{1}{mn}\sum_{x=0}^{m-1}\sum_{g=0}^{n-1}(f(x,g)-\hat{f}(x,g))^2 \tag{3.2}$$

where mn is the length of our image (number of pixels) which m represents the row and n represents the number of columns, $f(x,g)$ is our original image and $\hat{f}(x,g)$ is the estimated $f(x,g)$ [10].

Chapter 4

DE-NOISING BASED ON UN-DECIMATED WAVELET TRANSFORM USING IMPROVED SOFT THRESHOLDING TECHNIQUE

4.1. Introduction

Translation variance and poor directional properties are disadvantageous of DWT, so to solve this problem Stationary Wavelet Transform is presented as translation invariant wavelet transform. This type of wavelet transform is not performing down-sampling. [30], [31] represented a trous algorithm to determine UWT.

Besides, at each level of this wavelet transform, high and low pass filters will be operated and it is followed by obtaining 2 new sequences which have the same length as original. In this wavelet transform, we do not have up-sampling and down sampling. Figure 4.1 shows un-decimated wavelet transform for three levels where g(n) is low pass filter and h(n) is high pass filter. In this figure, after each level we obtain coefficients called detail and approximation. In addition, we are not losing high frequencies but keeping them. That is why the length of the output after each level is the same as the length of original input one.

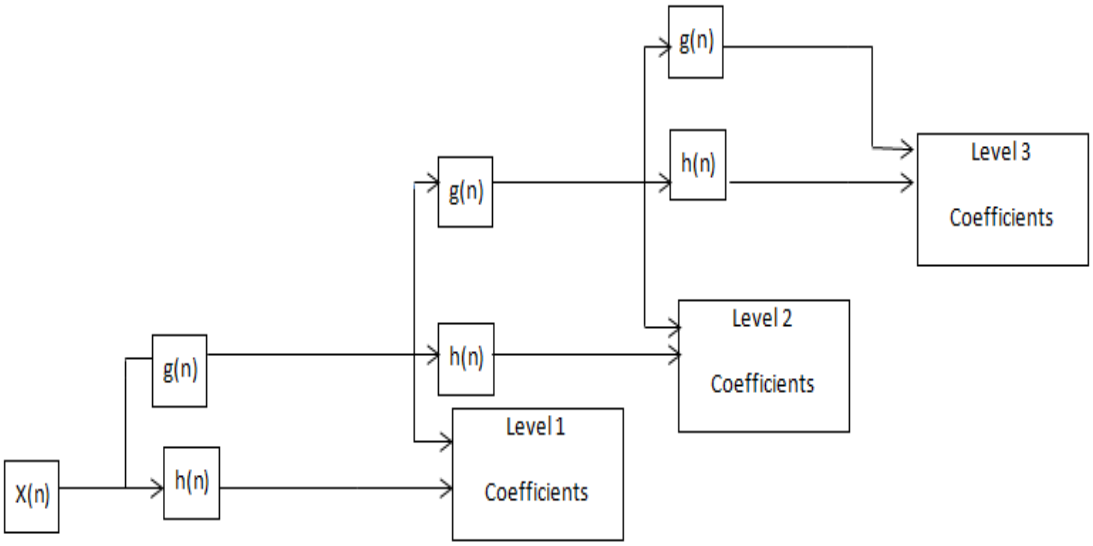

Figure 4.1: Stationary Wavelet Transform for Three Levels [32].

This wavelet transform is called un-decimated wavelet transform because there is not any decimation here [33], furthermore; we observe over-complete representation (at each level we have more outputs) instead of decimation [34] according to Coifman and Donoho's Proposed method on translation invariant de-noising [35]. This wavelet transform is also known as Redundant Wavelet Transform. Based on this concept, in the figure above, at first we have original signal and by passing through high pass and low pass filter in first level, it will be divided into 2 sequences as scaling (approximation) coefficients and detail coefficients. In the second level, the scaling coefficients from first level will be divided into 2 sequences again. By increasing the level of decomposition, this process will continue.

Here in the first contribution we see de-noising based on 2D and 3D versions of UWT combined with hard and soft thresholding and in the second contribution, application of improved soft thresholding on 3D-UWT is proposed to improve the results in terms of PSNR.

4.2 De-noising Based on UWT

In chapter 2, DWT has been applied on noisy image to process image de-noising. As it was mentioned before there were some problems using DWT like being shift or translation variance, so a wavelet transform is needed to cover the lack of translation invariance. To find a solution for this problem, UWT is suggested to use to meet that need. Here 2D and 3D-UWT joined with soft and hard thresholding methods have performed for de-noising procedure.

Figure below shows a general block diagram of de-noising methods. In this figure, two methods are proposed for de-noising in this chapter. In Figure 4.2 we can see UWT which has applied on input noisy image. Then in (a) we see de-noising based on 2D-UWT accompanied by hard and soft thresholding and in (b) we observe de-noising based on 3D-UWT combined with hard and soft thresholding as well. If we compare performance analysis of (a) and (b), we will find out that de-noising based on 3D-UWT using soft thresholding outperforms other methods such as 3D-UWT using hard, 2D-UWT using soft and 2D-UWT using hard thresholding function, so method 2 using soft thresholding gives the best result.

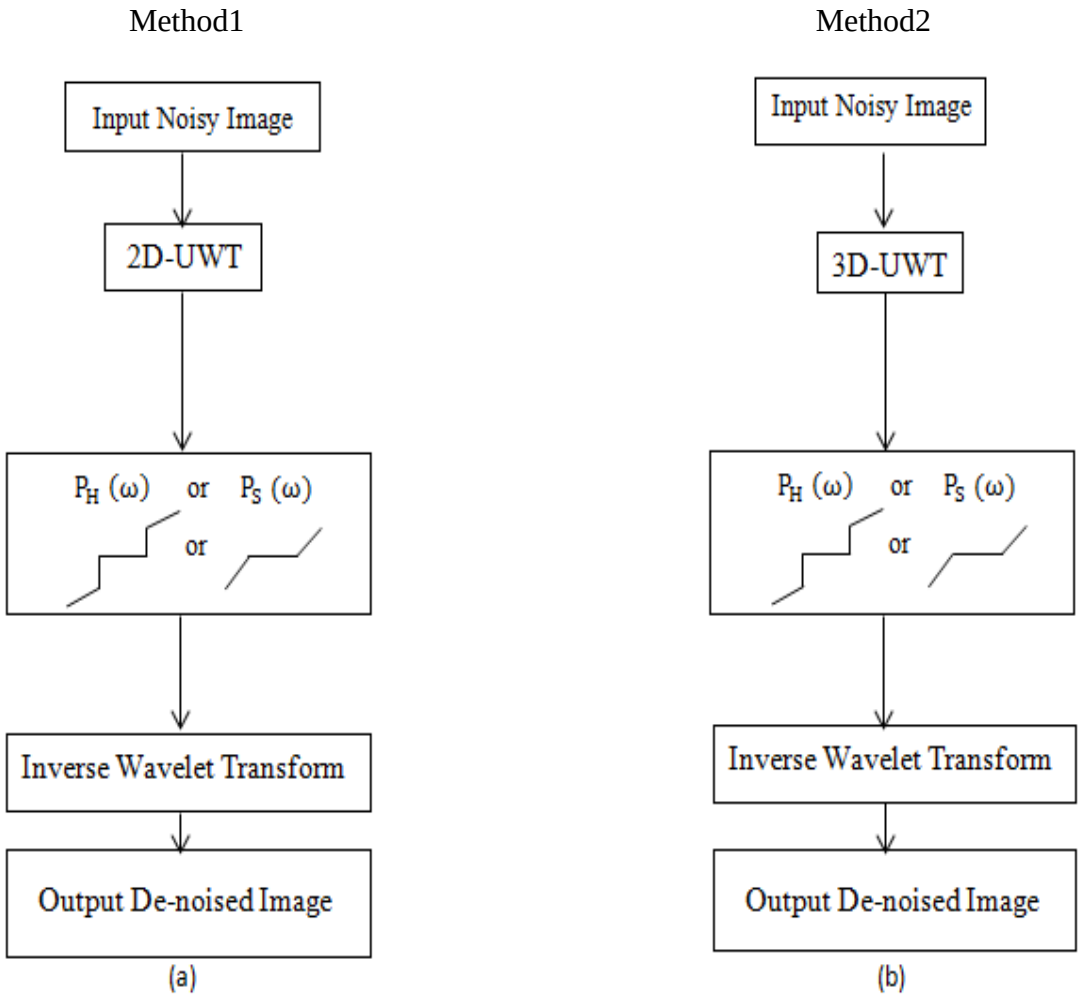

Figure 4.2: General Block Diagram of Proposed De-noising Methods.

4.3 Performance Analysis Based on UWT Using Hard and Soft Thresholding

In the first experiment, Indian pine hyper-spectral image is used to analyze de-noising using UWT for both 2D and 3D versions with hard and soft thresholding techniques. Our original image is band 25 of Indian Pine data set and we apply White Gaussian Additive Noise with zero mean and standard deviation of 20 to obtain a noisy version of original image with PSNR=21.98db. This process is followed by applying 2D and 3D versions of UWT with hard and soft thresholding techniques. Figure 4.3 (a) shows original band 25 of Indian Pine, (b) shows noisy image with

PSNR of 21.98 dB, in (c) we can see de-noised image based on 2D-UWT using hard thresholding with PSNR value of 28.38 dB and finally in (d) de-noised image based on 3D-UWT with hard thresholding is shown with PSNR of 29.25 dB. Based on the results obtained in Figure 4.3, it is clear that (d) performs better than (c) according to the higher PSNR value.

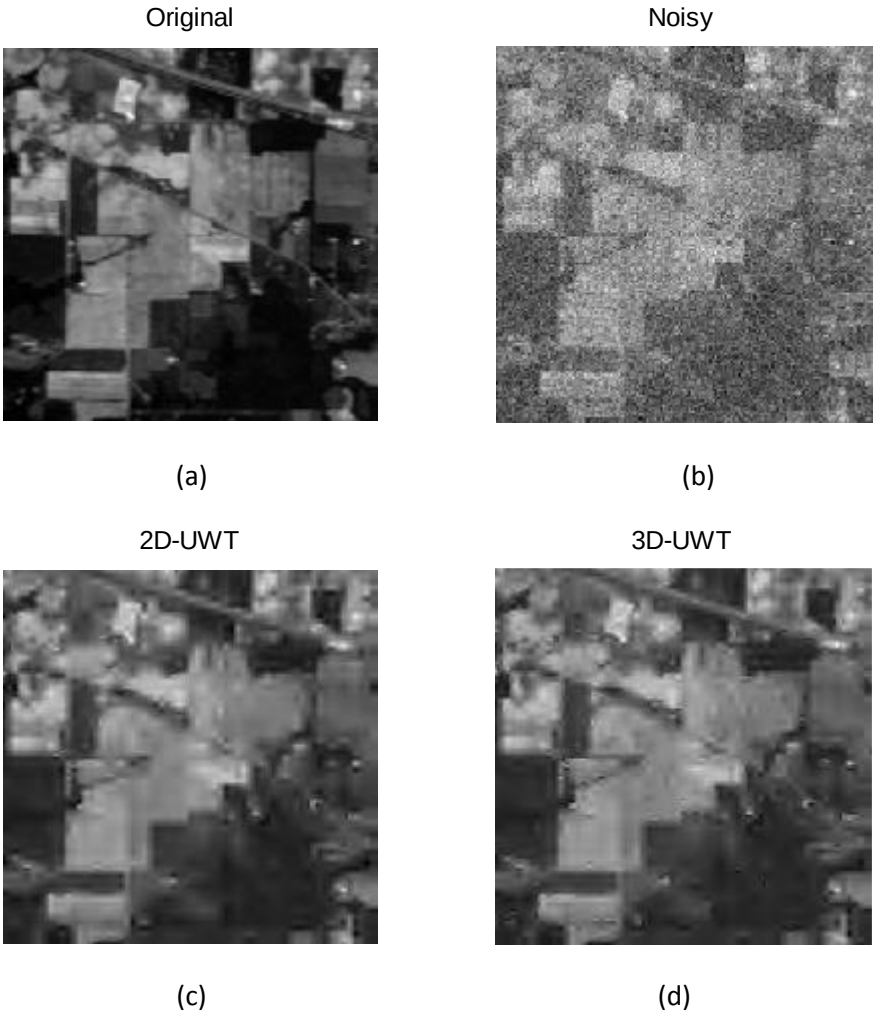

Figure 4.3: Indian Pine Hyper-spectral Image De-noising Based on UWT with Hard Thresholding Technique.

Figure 4.4 shows Indian Pine hyper-spectral image de-noising based on soft thresholding technique for 2D-UWT and 3D-UWT. In this figure, (a) is the original band 25 of Indian Pine, (b) is noisy image with PSNR of 21.98dB and (c), (d) are de-noised images using soft thresholding based on 2D-UWT and 3D-UWT,

respectively. Here for 2D-UWT the amount of PSNR is equal to 29.14 dB and for 3D-UWT it is equal to 30.55 dB, so 3D-UWT outperforms the 2D one because of the higher PSNR value.

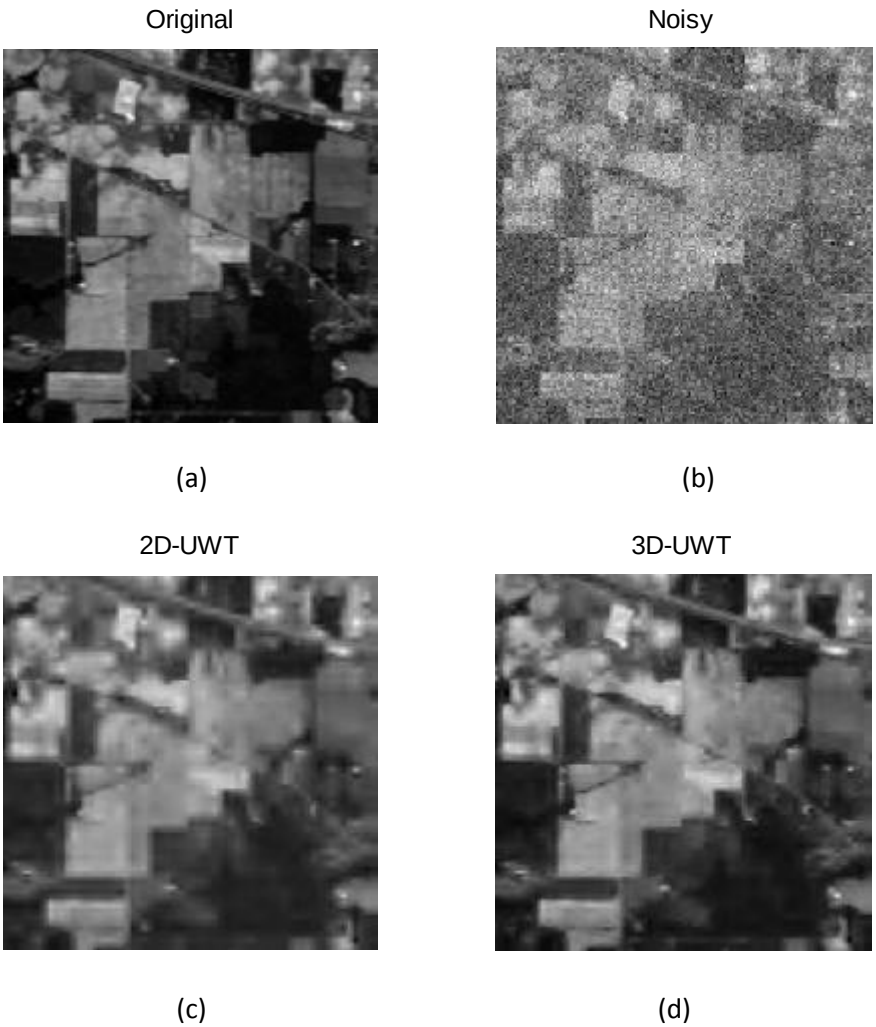

Figure 4.4: Indian Pine Hyper-spectral Image De-noising Based on UWT with Soft Thresholding Technique.

In the second experiment, Indian Pine data set has been used in different tables and graphs to analyze de-noising based on UWT using hard and soft thresholding. Table 4.1 shows experimental result for de-noising using 2D and 3D-UWT with hard thresholding technique. This table shows PSNR value for band 25, average of 10 experiments, average of all bands and average of between (20-28) bands. Based on

this table, if we compare de-noised results based on 2D-UWT and 3D-UWT, we will find out that PSNR values obtained with 3D-UWT are more than PSNR values acquired with 2D-UWT, so 3D version of UWT is better than 2D one for de-noising.

In Figure 4.5 we can see PSNR values vs different number of bands for noisy image, de-noised with 2D-UWT based on hard thresholding and de-noised with 3D-UWT based on hard thresholding as well. In this figure we observe that the average of PSNR value for bands (20-28) based on 2D-UWT is 28.62 dB while this average for 3D-UWT is 29.12 dB. According to what is mentioned, 3D-UWT is better than 2D-UWT.

Table 4.1: The Result of De-noising the Indian pine Hyper-spectral Image Using Hard Threshold for Band 25.

PSNR(dB)	Additive Gaussian Noise (σ=20,zero mean)	2D-UWT	3D-UWT
		Hard Thresholding	Hard Thresholding
Indian Pine for band 25	21.98	28.38	29.25
Average of 10 experiments	21.83	28.26	29.15
Average of all bands	22.02	27.73	28.42
Average of 8 bands(20-28)	22.10	28.62	29.12

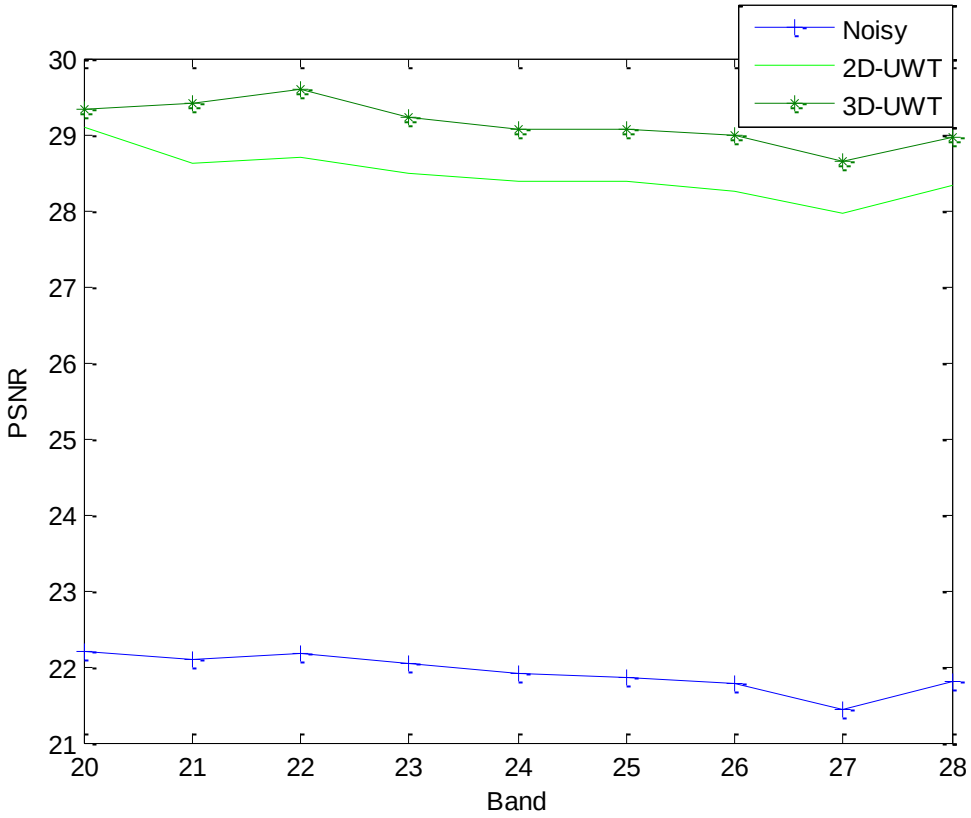

Figure 4.5: The PSNR Values vs Band for the Indian Pine Hyper-spectral Image (bands 20-28) Using Hard Thresholding.

Table 4.2 shows experimental result for de-noising using 2D and 3D-UWT with soft thresholding technique. This table indicates PSNR value for band 25, average of 10 experiments, average of all bands and average of bands (20-28) which these values for 2D-UWT are 29.14 dB, 29.10 dB, 29.35 dB and 29.56 dB, respectively and for 3D-UWT are 30.55 dB, 30.22 dB, 30.19 dB and 30.23 dB, respectively. After comparing these values we will see de-noising based on 3D-UWT outperforms 2D-UWT. In addition, in Figure 4.6 we can see PSNR values vs different number of bands for noisy image, de-noised with 2D-UWT based on soft thresholding and de-noised with 3D-UWT based on soft thresholding.

Table 4.2: The Result of De-noising the Indian Pine Hyper-spectral Image Using Soft Threshold for Band 25.

PSNR(dB)	Additive Gaussian Noise (σ=20,zero mean)	2D-UWT	3D-UWT
		Soft Thresholding	Soft Thresholding
Indian Pine for band 25	21.98	29.14	30.55
Average of 10 experiments	21.83	29.10	30.22
Average of all bands	22.02	29.35	30.19
Average of 8 bands(20-28)	22.10	29.56	30.23

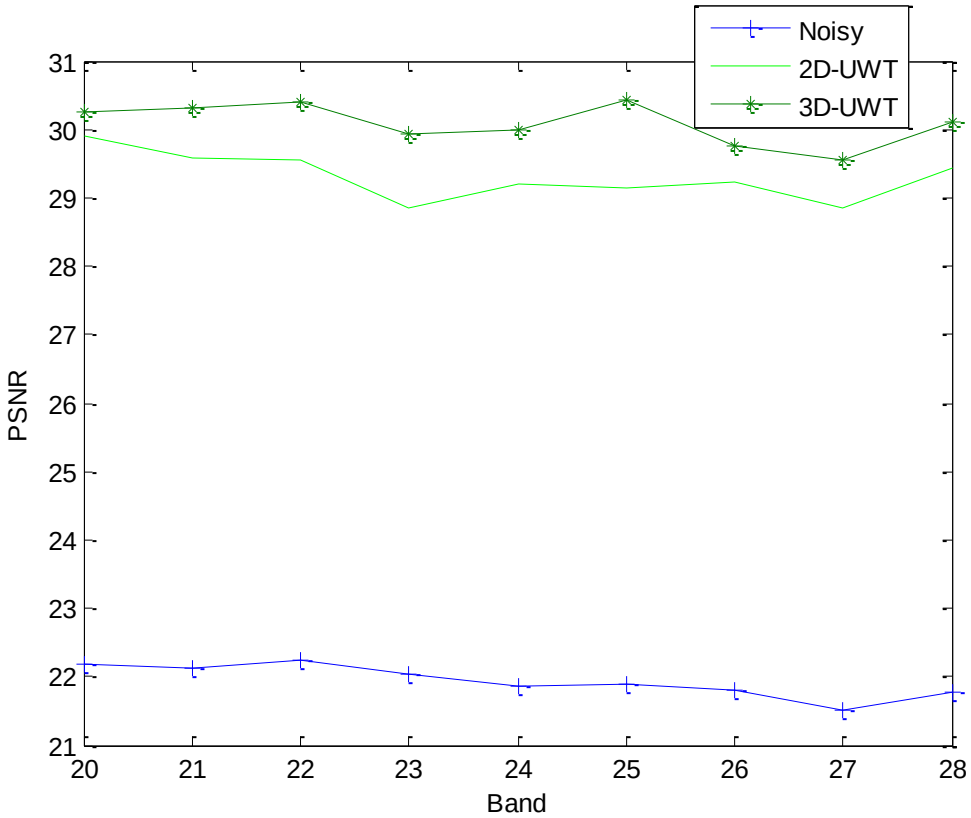

Figure 4.6: The PSNR Values vs Band for the Indian Pine Hyper-spectral Image (bands 20-28) Using Soft Thresholding.

In the third experiment Washington DC Mall, Pavia Canter and Pavia University have been used in two tables to analyze de-noising based on UWT using hard and soft thresholding. Here for all data sets mentioned above, PSNR values for 3D-UWT stay higher than 2D-UWT for both hard and soft thresholding techniques, moreover; soft thresholding performs better than hard in terms of PSNR value.

Table 4.3: Hyper-spectral Image De-noising Based on 2D and 3D-UWT Using Hard Thresholding for 10 Experiments of Band 25.

PSNR(dB)	Additive Gaussian Noise (σ=20,zero mean)	2D- UWT	3D- UWT
		Hard Thresholding	Hard Thresholding
Washington DC Mall	22.25	30.12	30.74
Pavia Center	22.95	28.56	30.78
Pavia University	21.95	27.98	29.69

Table 4.4: Hyper-spectral Image De-noising Based on 2D and 3D- UWT Using Soft Thresholding for 10 Experiments of Band 25.

PSNR(dB)	Additive Gaussian Noise (σ=20,zero mean)	2D- UWT	3D- UWT
		Soft Thresholding	Soft Thresholding
Washington DC Mall	22.25	31.10	31.67
Pavia Center	22.95	31.78	33.74
Pavia University	21.95	31.57	33.62

Here 2D and 3D versions of Un-decimated Wavelet Transform combined with hard and soft thresholding techniques have introduced to overcome some disadvantageous of DWT. In these experiments PSNR value has been obtained for one specific band (band 25) for de-noising based on 2D and 3D-UWT using hard and soft thresholding. In addition, average of PSNR values have been acquired as well for some experiments of band 25, a range of 8 specific bands (20-28) and all bands based on the mentioned de-noising methods. Among all the methods introduced above, 3D-UWT using soft thresholding holds highest PSNR value.

In the following section, we proposed a method which can enhance the PSNR value and improve the visual inspection as well. In this technique, we used a nonlinear soft threshold function and combined this function with 3D-UWT.

4.4 Improved Soft Thresholding

Improved soft threshold is higher order soft threshold function or smooth nonlinear soft threshold function. Being continuous, nonlinear and having smooth characteristic are its properties. (4.1) denotes the general formula for this function [36].

$$T_I(\omega) = \begin{cases} \omega + T - \frac{T}{2k+1} & , \quad \omega < -T \\ \frac{1}{(2k+1)T^{2k}}\omega^{2k+1} & , \quad |\omega| \leq T \\ \omega - T + \frac{T}{2k+1} & , \quad \omega > T \end{cases} \tag{4.1}$$

where $T_I(\omega)$ is Improved Soft Thresholding Function, ω is wavelet coefficients, T is threshold value and k is the degree of the function $(0 < k < \infty)$. With respect to this k value, we will have a smooth area between original signal and soft threshold function. For k=0 we have the following function which is actually the original signal.

$$T_I(\omega) = \begin{cases} \omega \ , & \omega < -T \\ \omega \ , & |\omega| \leq T \\ \omega \ , & \omega > T \end{cases} \tag{4.2}$$

For k=∞ we have the formula bellow which is soft thresholding function.

$$T_I(\omega) = \begin{cases} \omega + T \ , & \omega < -T \\ 0 \ , & |\omega| \leq T \\ \omega - T \ , & \omega > T \end{cases} \tag{4.3}$$

Based on what is mentioned above, for $k = 0$ and $k = \infty$ we have original and soft threshold function, respectively. In this way for $0 < k < \infty$ we observe higher order smooth curves called as improved threshold function. In addition, when the amount of k approaches to infinity our function will be much more smoothed as following.

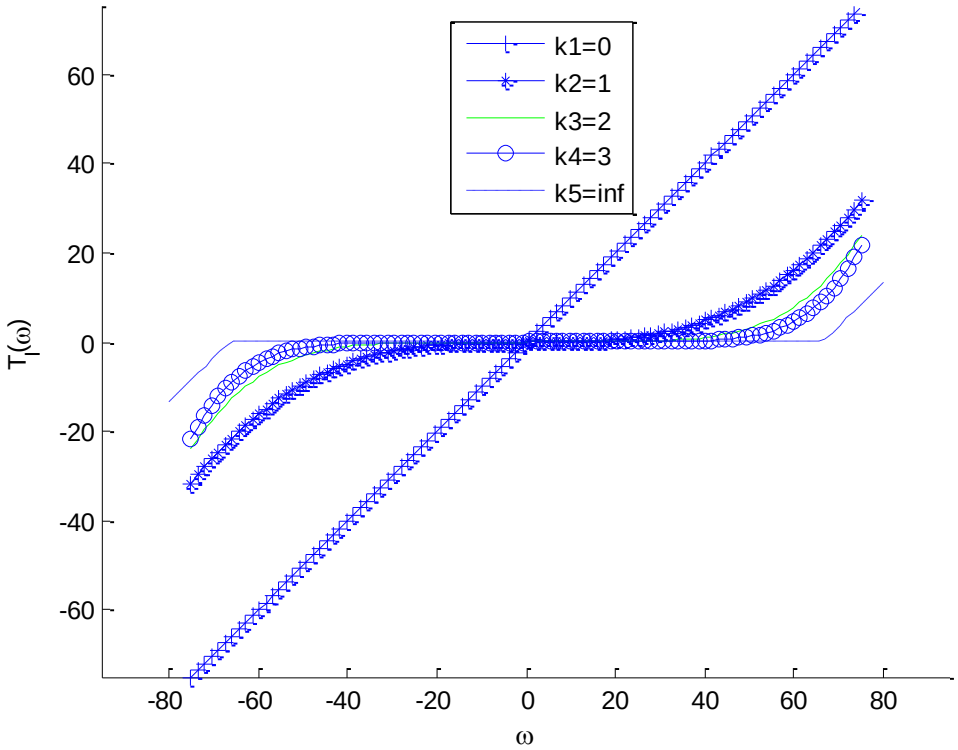

Figure 4.7: Improved Soft Threshold Functions vs Wavelet Coefficients for Different Values of k.

Figure 4.7 shows improved soft threshold function vs wavelet coefficients for $k = 0,1,2$ and infinity. It is clear that when the amount of k is increasing, the figure is approaching to soft thresholding function. A plus point is that, among different values of k, we should find an optimal value under this condition that with respect to this value, we will get highest PSNR. In Figure 4.8 different values of k has tried and $k = 1$ is chosen as the optimal value because it provides us with highest Peak Signal to Noise Ratio (PSNR). The following figure is for average of 100 images.

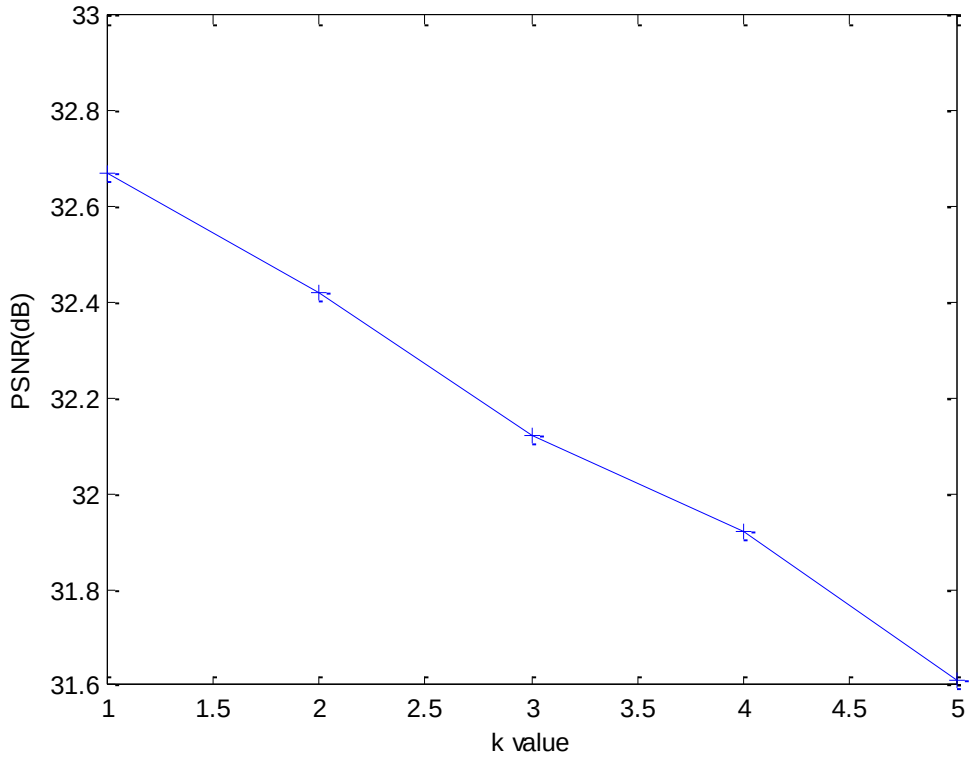

Figure 4.8: PSNR vs Different Values of k.

In Figure 4.9 we see hard threshold, soft threshold and improved soft thresholding function in one graph where x-direction is wavelet coefficients called ω and y-direction is threshold function (hard, soft and improved soft threshold function) called $T(\omega)$.

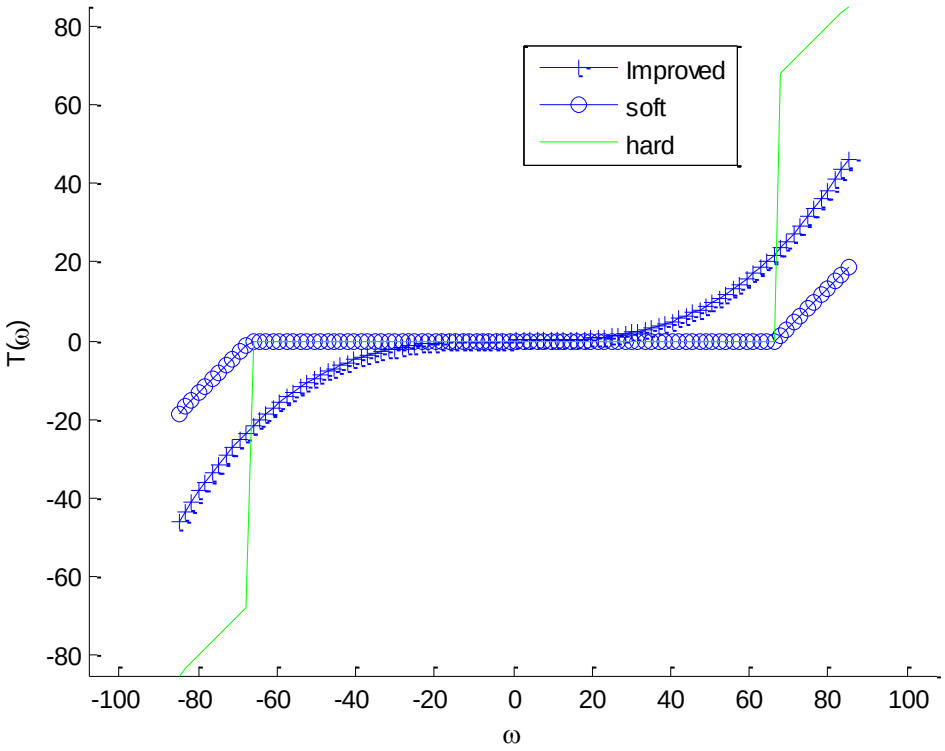

Figure 4.9: Hard, Soft and Improved Soft Threshold Functions vs Wavelet Coefficients for Different Values of k.

4.5 Performance Analysis Based on 3D-UWT with Improved Soft Threshold

Here in the first experiment, band 25 of Indian Pine Hyper-Spectral image and Gulf hyper-spectral image have used to analyze de-noising process. In addition, improved soft thresholding method has applied to 3D-UWT to improve the visual inspection and PSNR value. Figure 4.10 (a) shows de-noised image based on 3D-UWT using soft threshold and in (b) we can see de-noising based on 3D-UWT using improved soft thresholding method. In this figure, the PSNR value obtained with 3D-UWT

using soft threshold in (a) is 30.55 dB and PSNR value obtained with proposed method in (b) is 32.67 dB. It means that proposed method improved PSNR value for 2.12 dB.

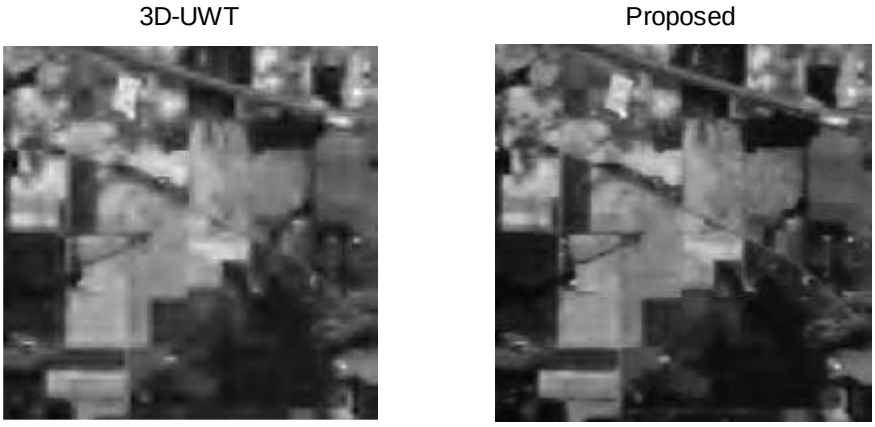

Figure 4.10: Indian Pine Hyper-spectral Image De-noising Based on 3D-UWT with Soft and Improved Soft Thresholding.

In the second experiment, Gulf of Mexico and Arizona Mining hyper-spectral image have been used to analyze de-noising process. In addition, improved soft thresholding method has applied to 3D-UWT to improve the visual inspection and PSNR value. Figure 4.11 shows de-noising based on 3D-UWT using soft threshold and proposed method for Gulf of Mexico data set and Arizona Mining hyper-spectral image. In this figure, the left column represented as (a), (c) are de-noised images based on 3D-UWT using soft thresholding and the PSNR values which have been obtained here are 30.95 dB for Gulf of Mexico hyper-spectral image in (a) and 30.42 dB for Arizona Mining data set in (c). In addition, the right column denoted as (b), (d) are de-noised images based on proposed method and PSNR values which have been acquired here are 32.12 dB for Gulf of Mexico data set in (b) and 31.88 dB for Arizona Mining image in (d). It means that proposed method improved PSNR value in both images.

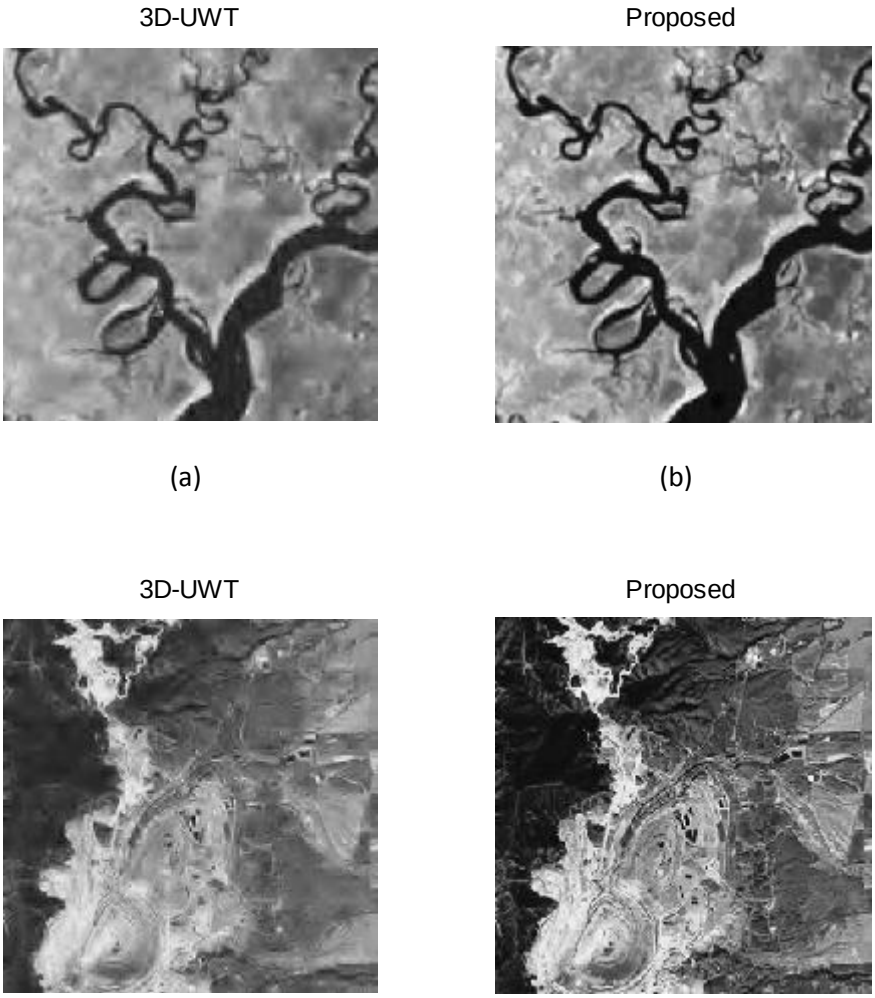

Figure 4.11: Image De-noising Based on 3D-UWT with Soft and Improved Soft Thresholding Technique.

In the third experiment Indian Pine hyper-spectral data set has used to see performance analysis of de-noising in a table and graph. In this experiment, 3D-UWT is used for de-noising based on soft and improved soft thresholding technique and proceeding figure represents the results obtained in this table.

Table 4.5 shows performance analysis of 3D-UWT using soft and improved soft threshold based on image de-noising. In this table, improved soft threshold combined with 3D-UWT is used as proposed method. Here experimental results have done based on PSNR vs band 25 of Indian Pine data set, average of 10 experiments for band 25, average of all bands and average of 8 bands between (20-28).

Table 4.5: The Result of De-noising the Indian Pine Hyper-spectral Image Using Soft Threshold and Improved Soft Threshold Method.

PSNR(dB)	Additive Gaussian Noise (σ=20,zero mean)	3D-UWT Soft Thresholding	3D-UWT Improved Soft Thresholding
Indian Pine for band 25	21.98	30.55	32.67
Average of 10 experiments	21.83	30.22	32.51
Average of all bands	22.02	30.19	32.28
Average of 8 bands(20-28)	22.10	30.23	32.12

In figure below we see PSNR values vs bands for noisy image, de-noised with 3D-UWT using soft thresholding and de-noised with proposed method. It is clear that the average of PSNR for 3D-UWT using soft threshold is 30.23 dB and for proposed method is 32.12 dB. It means that proposed method for de-noising performs better than 3D-UWT using soft thresholding because of holding highest PSNR value and visual resolution.

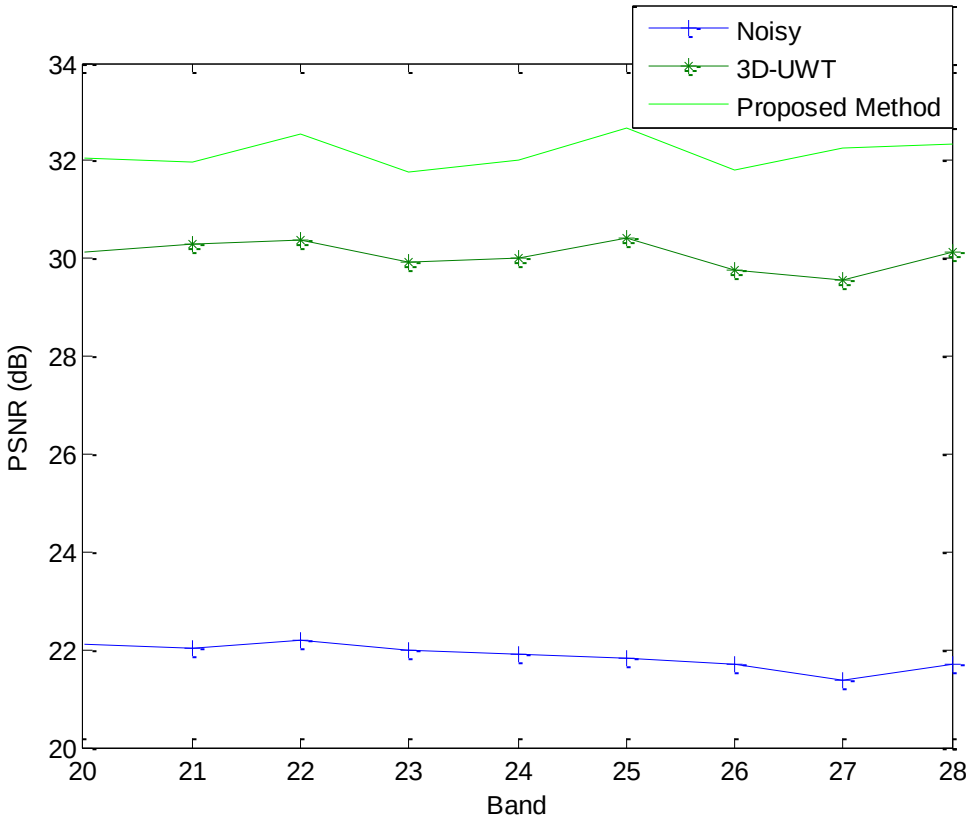

Figure 4.12: The PSNR Values vs Band for 3D-UWT and Proposed Method for Indian Pine Hyper-spectral Image (bands 20-28).

In the fourth experiment several hyper-spectral data sets like Washington DC Mall, Pavia Center and Pavia University used in the following table to analyze de-noising process. In this experiment de-noising based on 3D-UWT using soft and improved soft thresholding techniques have used. After comparing the results, we will find out that for all the data sets used in this experiment, proposed method outperforms 3D-UWT using soft thresholding in terms of PSNR value.

Table 4.6: The Result of Hyper-spectral Image De-noising Based on UWT Using Soft and Improved Soft Thresholding for 10 Experiments of Band 25.

PSNR(dB)	Additive Gaussian Noise (σ=20,zero mean)	3D- UWT	3D- UWT
		Soft Thresholding	Improved Soft Thresholding
Washington DC Mall	22.25	31.67	32.24
Pavia Center	22.95	33.74	34.85
Pavia University	21.95	33.62	34.78

In this chapter, firstly 2D and 3D-UWT have been introduced for de-noising based on hard and soft thresholding methods in several experiments and we found out image de-noising based on 3D-UWT with soft thtresholding is better than 2D-UWT with soft, 2D-UWT with hard and 3D-UWT with hard as well.

Secondly, improved soft thresholding technique has been proposed to improve the result in terms of PSNR value and resolution. In this way, we combined 3D-UWT with improved soft thresholding and we saw that average of PSNR values for all bands obtained by proposed method is 32.28 dB which is higher than PSNR values acquired with other methods used for de-noising in this thesis. In chapter 2, average

of PSNR values for all bands of Indian Pine data set based on 3D-DWT using soft thresholding method was 28.21 dB while proposed method improved this value to 32.28 dB, so it is better to process de-noising based on UWT using improved soft thresholding technique. Table 4.7 shows the performance of the proposed method (3D-UWT using improved soft threshold) in comparison with some other available methods. In this table, in the first column we can see the datasets which have been used during these experiments. Second column is some available methods. Third column is PSNRs based on applying those methods in second column on datasets which are mentioned in first column. As we can see in this table, Pastor's method [38] outperforms other methods. He used a nonlinear function in his experiment and this function performs very well in discarding noisy coefficients and keeping important features of image. In addition, nonlinearity, smoothness and continuity are the advantageous of this method.

Table 4.7: Evaluation of the PSNR Values for Different Available Hyper-spectral Image De-noising Methods.

Datasets	Methods	PSNR(dB)
Band 21 of WDM	Cubic Total Variation [16]	23.28
	3D-UWT Using Hard	27.56
	3D-UWT Using Soft	28.69
	3D-UWT Using Improved Soft(Proposed)	**29.32**
Bands (8-15) of Indian Pine Dataset (average of 10 experiments)	3D-Sar Using UWT [4]	29.90
	3D-UWT Using Hard	30.15
	3D-UWT Using Soft	31.22
	3D-UWT Using Improved Soft(Proposed)	**32.84**
Cuprite Mining	Framelet Transform Image De-noising [17]	28.77
	3D-UWT Using Hard	28.12
	3D-UWT Using Soft	29.14
	3D-UWT Using Improved Soft(Proposed)	**30.43**
Band 32 of WDM	Zhang's Method [18]	32.82
	3D-UWT Using Hard	30.89
	3D-UWT Using Soft	31.78
	3D-UWT Using Improved Soft(Proposed)	**33.44**
Band 25 of Indian Pine	Sahraeian's Method [37]	31.48
	3D-UWT Using Hard	29.25
	3D-UWT Using Soft	30.55
	3D-UWT Using Improved Soft(Proposed)	**32.67**
Band 12 of Pavia Center	Pastor's Method[38]	**33.68**
	3D-UWT Using Hard	30.25
	3D-UWT Using Soft	31.45
	3D-UWT Using Improved Soft(Proposed)	32.12

Chapter 5

CONCLUSION

5.1 Conclusion

As it is mentioned in previous chapters, a hyper-spectral image can be captured by different sensors like AVIRIS and ROSIS which provide us with a vast application in physics, engineering, chemistry, agriculture and also astronomy. These images can be influenced by noise, during the receiving process, so de-noising is an important work that should be done to enhance the visual inspection. De-noising based on wavelet transform is one of the common methods proposed recently. In this thesis, firstly, de-noising based on DWT using soft and hard thresholding methods have been used. Secondly, because of the lack of translation invariance, UWT is proposed using hard and soft thresholding techniques which we found out de-noising based on 3D-UWT using soft thresholding performs very well in comparison with 3D-UWT using hard, 3D-DWT using hard and soft and 2D-DWT using hard and soft. At the end, one method is proposed based on using a higher order application of soft thresholding function instead of using soft thresholding function. This function is called improved soft thresholding function. In this method, we applied this function to our image and then we found out that the de-noising results will be much more appealing.

According to what is cited above, we obtained our best de-noised image based on 3D-UWT combined with improved soft thresholding function. The proposed method improved the PSNR value and visual inspection pretty well.

5.2 Future Work

As de-noising is one of the most important works in image processing and the proposed function cannot be the only function to improve the result, so as my future work I will consider different type of thresholding functions such as sigmoid and exponential functions combined with wavelet transform to improve the resolution and the amount of PSNR value.

REFERENCES

[1] "What is Hyper-spectral Imaging," *http://www.hyspex.no/hyperspectral_imaging/,* November, 2008.

[2] "Hyper-spectral Imaging," *https://en.wikipedia.org/wiki/Hyperspectral_imaging*, November, 2016.

[3] "Light," *https://en.wikipedia.org/wiki/Light*, 2016.

[4] B. Rasti, J. R. Sveinsson, M. O. Ulfarsson and J. A. Benediktsson,"Hyper-spectral Image De-noising Using 3D Wavelets ," in *Proceeding of IEEE International Conference On Geoscience and Remote Sensing Symposium (IGARSS)*, pp. 1349-1352, July, 2012.

[5] "Image Noise," *http://www.sprawls.org/ppmi2/NOISE*

[6] A.K. Boyat and B.K. Joshi, "Noise Models in Digital Image Processing," *Signal and Image Processing: An International Journal (SIPIJ)*, Vol. 6, No. 2, April, 2015.

[7] "Additive white Gaussian noise," *https://en.wikipedia.org/wiki/Additive_white_Gaussian_noise,* December, 2016.

[8] D. Xu, L. Sun and J. Luo "De-noising of Hyper-spectral Remote Sensing Image Using Multiple Linear Regression and Wavelet Shrinkage." in *Proceedings of the*

International Conference on Information, Business and Education Technology (ICIBET), 2013.

[9] Y. Norouzzadeh and M. Rashidi. "Image De-noising in Wavelet Domain Using a New Thresholding Function," in *Proceeding of IEEE International Conference on Information Science and Technology*, pp. 721-724, 2011.

[10] L. Dong, "Adaptive Image De-noising Using Wavelet Thresholding." in *Proceeding of IEEE International Conference on Information Science and Technology*, pp. 854-857, 2013.

[11] B. Demir and S. Ertrk, "Improved Hyper-spectral Image Classification with Noise Reduction Pre-process," in *Proceedings of European Signal Processing Conference (EUSIPCO)*, 2008.

[12] A. A. Green, M. Berman, P. Switzer and M. D. Craig, "A Transformation for Ordering Multispectral Data in Terms of Image Quality with Implications for Noise Removal," *IEEE Trans. Geoscience and Remote Sensing*, Vol. 26, No. 1, pp. 65–74, 1988.

[13] G. Chen and S. Qian,"De-noising of Hyper-spectral Imagery Using Principal Component Analysis and Wavelet Shrinkage," *IEEE Trans. Geoscience and Remote Sensing*, Vol. 49, pp. 973–980, 2011.

[14] D.L. Donoho, I.M. Johnstone, ''Ideal Spatial Adaptation by Wavelet Shrinkage'', *Biometrika*, Vol. 81, pp. 425-455, 1993.

[15] E. Anisimova, J. Bednář and P. Páta. "Efficiency of Wavelet Coefficients Thresholding Techniques Used for Multimedia and Astronomical Image De-noising." in *Proceeding of IEEE International Conference On Applied Electronics (AE),* September, 2013.

[16] H. Zhang, "Hyper-spectral Image De-noising with Cubic Total Variation Model," *ISPRS Annals of the Photogrammetry, Remote Sensing and Spatial Information Science*, Vol. 1, No. 7, pp. 95-98, 2012.

[17] S. Sulochana, R.Vidhya, D.Vijayasekaran and K. Mohanraj, "De-noising and Dimensionality Reduction of Hyper-spectral Images Using Framelet Transform with Different Shrinkage Functions," *Indian Journal of Geo-Marine Science*, Vol. 45, No. 8, pp. 978-986, 2016.

[18] X. Zhang, "Thresholding Neural Network for Adaptive Noise Reduction," *IEEE Transactions on Neural Networks*, Vol. 12, No. 3, May, 2001.

[19] K. Rajpoot, N. Rajpoot and J. A. Noble, "Discrete Wavelet Diffusion for Image De-noising ," in *Proceeding of International Conference on Signal and Image Prosecing*, Vol. 5099, pp. 20-28.

[20] B. Ismail1 and A. Khan, "Image De-noising with a New Threshold Value Using Wavelets," *Journal of Data Science*, pp. 259-270, 2010.

[21] "Wavelet Tutorial," *http://web.iitd.ac.in/~sumeet/WaveletTutorial*

[22] “Discrete Wavelet Transform,” *https://en.wikipedia.org/wiki/Discrete_wavelet_transform*, November, 2016

[23] L. Lei, C. Wang and X. Liu, “Discrete Wavelet Transform Decomposition Level Determination Exploiting Sparseness Measurement ,” *International Journal of Electrical, Computer, Energetic, Electronic and Communication Engineering* , Vol. 7, No. 9, 2013

[24] K. Cho, Y. You and K. Eshraghian, “Three-Dimensional Discrete Wavelet Transform (DWT) Based On Unary Arithmetic ,” Chungbuk National University, College of Electrical and Computer Engineering, January, 2010.

[25] “Matlab Implementation of Wavelet Transforms,” *http://eeweb.poly.edu/iselesni/WaveletSoftware/standard3D.html*

[26] B. Ismail1, “Image De-noising with a New Threshold Value Using Wavelets,” *Journal of Data Science,* pp. 259-270, 2010.

[27] D. L. Donoho, “De-noising by Soft Thresholding.” *IEEE Trans. Information Theory*, vol. 41, pp. 613-627, 1995.

[28] “Advanced Hyper-spectral and Geospatial Solution,” http://www.spectir.com/free-data-samples/, 2010

[29] “Imaging in Both Visible and Shortwave Infrared Spectrums to Collect More Information with Hyper-spectral Imaging,” http://www.sensorsinc.com/applications/military/hyperspectral-imaging

[30] A. Gyaourova, C. Kamath and I. K. Fodor. “*Un-decimated wavelet transforms for image de-noising*,” University of Nevada, November, 2002.

[31] M. Holschneider, R. Kronland-Martinet, J. Morlet, and P. Tchamitchiam,“A real-time algorithm for signal analysis with the help of the wavelet transform,” *Wavelets, Time-Frequency Methods and Phase Space*, pp. 289–297, 1989.

[32] “Stationary Wavelet Transform,” *https://en.wikipedia.org/wiki/Stationary_wavelet_transform*, August, 2016.

[33] Advanced Signal Processing Toolkit, “Un-decimated Wavelet Transform” *http://zone.ni.com/reference/en-XX/help/371419D01/lvasptconcepts/wa_uwt/*, June, 2010

[34] M. Tomic, “Adaptive Wavelet Transforms with Application in Signal De-noising,”

[35] R. R. Coifman and D. L. Donoho,’’ Translation-invariant de-noising,’’ in *Wavelet and Statistics, Springer Lecture Notes in Statistics 103*, New York, Springer-Verlag, pp. 125-150, 1995.

[36] D. Ren and H. Haeri, “Advanced Material Science and Engineering,” in *Proceedings of the International Conference on Advanced Material Science and Engineering*, January, 2016.

[37] S. M. E. Sahraeian, F. Marvasti and N. Sadati, “Wavelet Image De-noising Based on Improved Thresholding Neural Network and Cycle Spinning,” in *Proceeding of IEEE International Conference on Acoustics, Speech and Signal Processing*, pp.585-588, 2007.

[38] A. M. Atto, D. Pastor and G. Mercier, “Wavelet Shrinkage: Unifcation of Basic Thresholding Functions and Thresholds,” *Signal, Image and Video Processing, Springer Verlag*, Vol. 5, No.1, pp. 11-28, 2011.